NACA

RESEARCH MEMORANDUM

INVESTIGATION OF COMBUSTION IN 16-INCH RAM JET UNDER SIMULATED CONDITIONS OF HIGH ALTITUDE AND HIGH MACH NUMBER

By T. J. Nussdorfer, D. C. Sederstrom
and E. Perchonok

Lewis Flight Propulsion Laboratory
Cleveland, Ohio

NATIONAL ADVISORY COMMITTEE
FOR AERONAUTICS

WASHINGTON

June 27, 1950

NATIONAL ADVISORY COMMITTEE FOR AERONAUTICS

RESEARCH MEMORANDUM

INVESTIGATION OF COMBUSTION IN 16-INCH RAM JET UNDER SIMULATED CONDITIONS OF HIGH ALTITUDE AND HIGH MACH NUMBER

By T. J. Nussdorfer, D. C. Sederstrom and E. Perchonok

SUMMARY

A connected-pipe investigation of a 16-inch ram jet was conducted in the Lewis altitude wind tunnel under controlled conditions of combustion-chamber-inlet pressure and temperature, fuel flow, and nozzle-outlet area. Three flame holders (the serrated annular baffle, the rake, and the corrugated gutter) provided satisfactory performance.

The performance of all three flame holders was considerably influenced by the radial position of the fuel injector and the engine-outlet area. Gasoline proved a superior fuel to kerosene for both annular and rake burners. With the corrugated gutter burner, the data indicated that a blend by volume of 50-percent gasoline and 50-percent propylene oxide might be slightly superior to gasoline.

The maximum fuel-air ratio operating range (0.030 to above 0.098) was obtained with the rake burner using a split-injection fuel system. A maximum combustion efficiency of 85 percent was obtained with this burner. The corresponding total-temperature ratio τ was 5.8; the fuel-air ratio, 0.055; and the combustion-chamber-inlet velocity, 177 feet per second. Maximum τ values near 6.0 were obtained with both annular and rake burners.

At low combustion-chamber pressure better performance was obtained with the corrugated gutter burner than with either of the other burners. With gasoline as fuel, a peak combustion efficiency of 79 percent at a fuel-air equivalence ratio of 0.76 and a combustion-chamber-inlet velocity of 211 feet per second was obtained at a combustion-chamber-inlet static pressure of 800 pounds per square foot absolute. For a given configuration, only slight changes in the total-pressure ratio across the combustion chamber were obtained over the entire operating range.

[redacted]

[redacted]

INTRODUCTION

Usual investigations of full-scale ram jets divorce the supersonic diffuser from the engine by connecting the subsonic inlet directly to the air supply and, as such, are primarily burner tests. A pressure recovery is assumed for a supersonic diffuser and the engine performance is computed accordingly. From a small-scale ram-jet investigation in a supersonic wind tunnel (reference 1), however, the pressure recovery across the supersonic diffuser was found to be influenced by burner design and combustion-chamber performance. As a result of poor burning, oscillating inlet shocks that greatly reduce the diffuser pressure recovery may occur. Similar oscillating shocks have been encountered during a cold-flow diffuser investigation (reference 2). Pulsing of the exhaust of an expendable free-flight 16-inch ram jet has also been recently reported (reference 3). Although the pulsing exhibited in flight was believed to be caused by rough and unstable combustion, evaluation of the phenomenon was difficult because of limited instrumentation on the flight vehicle.

In order to provide information on the stability of combustion and its effects on the supersonic diffusion of a full-scale 16-inch ram-jet engine, connected-pipe and free-jet studies were made in the altitude wind tunnel at the NACA Lewis laboratory. The engine was first run connected directly to the air supply without a supersonic inlet to determine the limitations of various burner configurations. Results of the connected-pipe study presented herein summarize the performance of several burner configurations and fuels at high altitudes and Mach numbers simulated to correspond to those expected in the free-jet study. With the exception of some burner performance at very low combustion-chamber static pressures, all burner performance reported was obtained at ram pressure ratios greater than that required for a Mach number of 1 at the exhaust-nozzle outlet. Combustion efficiency and gas total-temperature ratio are presented as a function of fuel-air ratio for three nozzle areas and a range of combustion-chamber static pressures. The effect of changes in the gas total-temperature ratio on the total-pressure ratio across the combustion chamber is also presented.

APPARATUS

The ram jet was supported above a wing spanning the wind-tunnel test section and attached to the tunnel balance frame (fig. 1). Atmospheric air, which was dried and then heated, was drawn into the engine through a make-up air duct by raising the

test-section altitude. A valve in this duct provided means for setting the engine static pressure at any value between atmospheric pressure and the tunnel ambient pressure. With no throttling of the inlet air, pressure ratios equivalent to free-stream Mach numbers somewhat in excess of 1.7 could be obtained. The ram jet exhausted directly into the tunnel test section. A 14-inch-diameter slip joint separated the engine from the ram pipe and made possible the use of the tunnel scales for thrust measurements.

Ram jet. - The ram jet (fig. 2) used in this investigation consists of a subsonic annular diffuser, a water-cooled combustion chamber 16 inches in diameter, and a water-cooled nozzle with an area that could be varied by a movable plug mounted within the combustion chamber. (The movable plug is described in reference 4.) The diffuser was fabricated of 1/8-inch-thick steel, whereas the combustion chamber, the tail plug, and the nozzle were made of 16-gage Inconel.

The over-all length of the engine from the inlet of the subsonic portion of the diffuser to the nozzle outlet is 175 inches, of which the combustion chamber and the nozzle comprise 90 inches. Coordinates for the center body and the ram-jet shell are given in table I. A transition piece was employed to reduce the slip-joint diameter from 14 to 9.92 inches at the subsonic-diffuser inlet. The diffuser center body projected 8 inches into the transition piece and the downstream end terminated at the combustion-chamber inlet with a pilot burner. The nose of the center body consisted of a 46° spike designed with an axial travel of 2 inches for subsequent free-jet studies. The spike was retained in the fully retracted position for this investigation. Variation of the flow area through the diffuser is given in figure 3. Irregularities in the curve are caused by center-body supporting struts whose maximum thicknesses never exceed 17 percent of the chord length. Three equally spaced struts were used at both front and rear support points.

Pilot system. - A vortex pilot patterned after the system described in reference 5 was housed in the downstream end of the center body (figs. 2 and 4). The pilot combustion chamber consisted of a truncated cone 10.3 inches long that changed in diameter from $7\frac{1}{4}$ inches at the upstream end to 6 inches at the exit. Propylene oxide in amounts not exceeding 5 percent of the total fuel flow was burned in the pilot. A single fuel nozzle rated at 21.5 gallons per hour at a pressure differential of 100 pounds per square inch was used. Air was scooped from the main air supply at two of the

three main center-body supports and ducted into the pilot through elbows, which imparted a vorter motion to the air. The fuel was ignited with a commercial jet-engine spark plug.

Fuel-injection system. - The fuel injector was located 17 inches upstream of the flame holder. A remotely controlled mechanism housed within the center body made possible the radial adjustment of the fuel injector during operation. Various types of fuel bar could be attached to four arms spaced 90° apart. These arms had a 2-inch radial adjustment in an annular passage 4 inches wide. Fuel was fed from a central manifold through flexible lines to the injector. The details of the system are shown in figure 4.

Two basic fuel-injection patterns were investigated. One pattern consisted of four arc segments making up a manifold to which four modified commercial spray nozzles were attached (fig. 5). The nozzles, rated at 21 gallons per hour at a differential pressure of 100 pounds per square inch, were modified by reducing the external cross-sectional area without affecting the spray pattern (fig. 6). The fuel was sprayed upstream at an injection radius that could be varied from 5.22 to 7.22 inches. The other pattern (fig. 7) consisted of four arc segments of 1/4-inch-diameter tubing, which had been flattened to reduce the blocking area. Twenty-five 0.028-inch-diameter orifices were drilled in each segment. Every third orifice sprayed radially inward and the others were directed upstream. In this case the fuel-injection radius could be varied from 5.38 to 7.38 inches. Special auxiliary injectors that were also used are described in the discussion of results.

Fuels. - The stoichiometric mixture ratios and the lower heating values of the fuels used in this investigation are as follows:

Fuel	Stoichiometric fuel-air ratio	Lower heating value (Btu/lb)
Gasoline, AN-F-48b, grade 80	0.067	19,000
Kerosene, AN-F-32a	.068	18,500
50-percent gasoline and 50-percent propylene oxide	.081	16,060

Flame holders. - All flame holders were mounted with the center rim around the pilot chamber exit. The serrated annular baffle and rake flame holders were made of 1/8-inch mild steel, whereas the corrugated gutter flame holder was made of 16-gage Inconel.

The serrated annular baffle flame holder (fig. 8) consisted essentially of an annular baffle set at 35° to the air stream with inner and outer diameters of 9.6 and 14.4 inches, respectively. Triangular serrations $2\frac{1}{4}$ inches deep were cut into the outer side. Nine 1-inch sweptback radial gutters connected the baffle to the center support rim. Provision was made for injecting fuel within the flame holder through nine commercial spray nozzles located opposite the radial connecting gutters. This flame holder had a projected blocking area of 55 percent of the annular combustion-chamber-inlet area.

The rake-type flame holder (fig. 9) was patterned after a flame holder described in reference 6. Each of the six rake clusters was attached to the supporting rim by a 90° radial gutter, $2\frac{1}{4}$ inches wide. Fuel was injected within each cluster through commercial spray nozzles. The blocking area of this flame holder was 41 percent of the annular combustion-chamber-inlet area.

The corrugated gutter flame holder (fig. 10) consisted of a series of corrugated gutters having a chord of 2 inches, a spacing of 1 inch between corrugations, and an angular gutter variation from 35° to 53° included angle. Smaller uncorrugated connecting gutters were welded between the corrugated sections. This flame holder had a blocking area of 54 percent of the annular combustion-chamber-inlet area.

The effect of variation in combustion-chamber-inlet Mach number on the cold total-pressure-drop coefficient for all three flame holders is shown in figure 11. Included in this coefficient are pressure losses in the combustion chamber and the nozzle, which are negligible in comparison with the flame-holder loss. Simple theory indicates that at a given Mach number the total-pressure-drop coefficient should increase with flame-holder blocking area (reference 7). The apparent inconsistency in the pressure-drop coefficients for the serrated annular baffle and corrugated gutter flame holders is explained by the fact that all the blocking of the annular flame holder does not occur in a single plane normal to the air flow and that the contraction coefficient is not the same for all flame holders.

Nozzle. - A hydraulically operated, movable, water-cooled plug was mounted in the last 6 feet of the combustion chamber. In the fully retracted position, the tip of the plug extended to the nozzle outlet. The plug, which has a maximum diameter of $8\frac{1}{16}$ inches, was

provided with an axial travel of 11.75 inches. The plug position was remotely controlled and could be changed while the engine was operating. The nozzle is a 9-inch truncated cone, tapering from the 16-inch combustion-chamber diameter to a 13.75-inch outlet diameter. At all plug positions, the minimum plane area occurred at the nozzle outlet. The variation of nozzle-outlet area with plug position in figure 12 shows that a variation in outlet area of 51 to 74 percent of the combustion-chamber area is possible. The ratio of the nozzle-outlet area to the 16-inch-diameter combustion-chamber area is hereinafter called the outlet-area ratio.

PROCEDURE

The engine was liberally instrumented with total- and static-pressure tubes and thermocouples. Pressures were read from photographs of manometer boards and temperatures were manually recorded from a self-balancing potentiometer. The air flow through the engine was calculated from pressure-rake data obtained at stations x and y (fig. 2). The combustion-chamber-inlet velocity was calculated from the wall static pressure at the combustion-chamber inlet and the measured air flow.

Data obtained with the tail rake (figs. 1 and 2), which retracted as the plug was extended, were used in obtaining the total pressure at the engine outlet. Combustion efficiency and gas total-temperature rise were computed by methods presented in references 8 and 9 from the measured jet thrust (with tunnel scales) and the air and fuel flows. The rate of fuel flow was measured with a rotameter calibrated for the fuel being used. The heat lost to the combustion chamber and the nozzle-plug cooling water as well as the energy content of the pilot fuel were included in the evaluation of combustion efficiency. In the evaluation of the final gas temperature and the ratio of absolute total temperature at nozzle outlet to absolute total temperature at combustion-chamber inlet, however, the heat lost to the cooling water was excluded.

In order to start the engine, the tunnel was first evacuated to the desired pressure altitude and the nozzle plug was positioned for a small outlet area. With a slight amount of air flow through the engine, the pilot was ignited. Burner ignition occurred when the proper proportion of fuel was added. Obtaining the desired operating conditions, however, required simultaneous regulation of fuel flow, air flow, and outlet area. The pilot was allowed to burn continuously. Burner performance and fuel-air ratio range were

determined at several engine-outlet areas, at pressure altitudes up to 50,000 feet, and at combustion-chamber static pressures expected in the free-jet investigation.

For each burner the optimum radial position for the fuel injector was determined in the following manner: At a fuel flow and nozzle-outlet area that gave typical engine operation, the radial position of the fuel injector was slowly varied from the retracted to the extended position. The position that gave the minimum combustion-chamber-inlet velocity (as determined with an airspeed indicator) was assumed to result in the maximum combustion efficiency and the maximum exhaust-gas temperature. For a given burner and fuel, the optimum fuel-injector position thus determined remained essentially constant for most operating conditions.

SYMBOLS

The following symbols are used in this report:

A	cross-sectional area, square feet
E	fuel-air equivalence ratio, ratio of actual to stoichiometric fuel-air ratio
f/a	fuel-air ratio
M	Mach number
P	total pressure, pounds per square foot absolute
p	static pressure, pounds per square foot absolute
q	dynamic pressure, pounds per square foot
T	total temperature, $^{\circ}R$
V	velocity, feet per second
η_b	combustion efficiency, percent (based on enthalpy change of gases and energy content of fuel injected)
τ	ratio of absolute total temperature at nozzle outlet to absolute total temperature at combustion-chamber inlet

[redacted]

Subscripts (fig. 2):

1	supersonic-diffuser inlet
2	subsonic-diffuser inlet
3	diffuser outlet and combustion-chamber inlet
4	combustion chamber
5	combustion-chamber outlet
6	nozzle outlet
f	fuel
x	air-flow measuring station
y	diffuser-inlet pressure-survey station

RESULTS AND DISCUSSION

The burner configurations investigated and the range of combustion-chamber-inlet variables over which they would operate are described in table II. The influence of the fuel-injection radius, the outlet-area ratio A_6/A_4, and the type of fuel burned on the operational performance of the three burners is also indicated. In general, only the configurations that resulted in relatively good performance are reported herein.

The fuel-injection radius was found to be critical to the performance of all the burners investigated. A change of 1/4 inch in injection radius could cause a serious reduction in combustion efficiency, rough and unstable burning, and in some instances flame blow-out. Data were obtained in most cases only at the injection radius for maximum performance.

The combustion-chamber-inlet velocities V_3 indicated in table II for which flame blow-out occurred were obtained by extrapolation from a plot of V_3 as a function of f/a to an estimated f/a at the blow-out point.

All data, except for a combustion-chamber-inlet static pressure p_3 of approximately 800 pounds per square foot absolute, were obtained with a choked outlet and therefore represent burner

performance whenever the existing combustion-chamber-inlet conditions can be duplicated.

Burner Performance with Serrated Annular Baffle Flame Holder

Operational performance. - Table II indicates that the best results were obtained with the annular flame holder when the orifice fuel injector (fig. 7) was used.

A fuel-injection radius of 6.22 inches (run 1) gave the best combustion performance and at an outlet-area ratio of 0.739 resulted in an operational f/a range of 0.053 to 0.092 with lean and rich blow-out velocities of 195 and 194 feet per second, respectively. When the outlet-area ratio was decreased to 0.676 and then further decreased to 0.600 (runs 2 and 3), the operable f/a range shifted toward the lean region, approximately 0.04 to 0.08. For all three outlet-area ratios, lean blow-out occurred at essentially the same V_3 (200 ± 5 ft/sec).

With all conditions identical to those of run 3 but with p_3 reduced to 1365 pounds per square foot absolute (run 4), rough burning or blow-out occurred at outlet-area ratios above 0.600. At an outlet-area ratio of 0.600, the reduction in combustion-chamber-inlet static pressure from 1750 to 1365 pounds per square foot absolute resulted in a decrease in the operable f/a range. In addition, this reduction in p_3 reduced V_3 at lean blow-out to 177 feet per second.

The annular burner was run with an injection radius of 5.38 instead of 6.22 inches to determine the effect of injection radius on burner performance (run 5, table II). With gasoline as fuel and a p_3 of 1800 pounds per square foot absolute, rough and unstable operation resulted at outlet-area ratios greater than 0.676. At this outlet-area ratio, the operable fuel-air ratio range was very narrow, 0.044 to 0.052.

With kerosene as fuel, best operational performance with the annular flame holder was obtained at a fuel-injection radius of 5.94 inches (as compared to 6.22 in. with gasoline). Results for an injection radius of 5.94 inches are shown only at a combustion-chamber-inlet pressure of 1790 pounds per square foot absolute (runs 6 to 8). At outlet-area ratios of 0.739 and 0.676, the

operable fuel-air ratio range was extremely narrow and lean blow-out occurred at mixtures near or richer than the stoichiometric value (0.068). Reducing the outlet-area ratio to 0.600 (run 8) approximately doubled the operable range and extended both rich and lean blow-out limits.

Although burning was attained with the fuel injected through commercial spray nozzles within the flame holder, the results were unsatisfactory and are not reported herein.

Effect of fuel-air ratio on burner performance. - The variation of combustion efficiency η_b and total-temperature ratio across the engine τ with f/a is shown in figure 13. Data were obtained with gasoline over a range of outlet-area ratios and at a combustion-chamber-inlet static pressure of 1750 pounds per square foot absolute. The maximum η_b of 82 percent was obtained at f/a of 0.054 and outlet-area ratio of 0.676. The corresponding V_3 was 180 feet per second. Operation at the largest outlet-area ratio (0.739) resulted in combustion efficiencies approximately 4 percent lower over the entire fuel-air ratio range than those obtained with the two smaller outlet-area ratios. For all outlet-area ratios, the maximum η_b occurred near an f/a of 0.054 and decreased at both the leaner and richer values. Maximum values of τ, however, were at f/a ratios richer than those at which the peak η_b was observed. The maximum τ of 6.0 was observed between f/a of 0.065 and 0.072 for the two smaller outlet-area ratios. Further increases in f/a caused a slight reduction in τ. At the largest outlet-area ratio (0.739), the maximum value of τ was 5.8 and occurred at f/a of 0.058 and V_3 of 189 feet per second.

Also shown in figure 13 are three data points obtained at a p_3 of 1365 pounds per square foot absolute and at an outlet-area ratio of 0.600. This pressure level is near that at which blow-out occurs for this burner. At outlet-area ratios greater than 0.600, burning was rough and unstable. A maximum η_b of 70 percent was obtained at a f/a of 0.051 and a V_3 of 168 feet per second. A maximum τ (5.8) resulted at a f/a of 0.066. The concomitant η_b was 68 percent and V_3 was 157 feet per second.

A comparison of the combustion performances obtained with kerosene and gasoline is made in figure 14. The curves for gasoline were taken from figure 13. The data obtained with kerosene at all three outlet-area ratios appear to fall on a single curve.

Although the maximum combustion efficiency of 66 percent occurred closer to the stoichiometric mixture (fuel-air equivalence ratio of 1) with kerosene than with gasoline, the combustion efficiencies and the resulting values of τ were consistently lower for kerosene. The maximum combustion-chamber-inlet velocity at which data were obtained with kerosene was 189 feet per second and the corresponding τ was 5.6.

Burner Performance with Rake Flame Holder

Operational performance. - With the rake flame holder (fig. 9) as with the annular flame holder, optimum performance (see table II) was obtained with the orifice fuel injector (fig. 7). With gasoline as fuel, a fuel-injection radius of 5.94 inches was required for optimum combustion-chamber performance. At a combustion-chamber-inlet static pressure of 1800 pounds per square foot absolute, decreases in the outlet-area ratio slightly extended the rich and lean operating limits (runs 9 to 11, table II). At the smallest outlet-area ratio (0.600), the operable f/a range was from 0.047 to 0.074.

With kerosene as fuel, the optimum mean fuel radius was found to be 5.74 inches (runs 12 and 13). The rich blow-out limit could not be determined because it was beyond the pumping capacity of the fuel system. At comparable outlet-area ratios, a greater operable range was obtained with kerosene than with gasoline. Satisfactory operation was obtained at combustion-chamber-inlet velocities in excess of 200 feet per second with both fuels. For an outlet-area ratio of 0.676 (run 12), lean blow-out occurred at approximately the same V_3 and f/a at 1850 pounds per square foot absolute as at 1470 pounds per square foot absolute.

In order to extend the operable f/a range in the lean region, the principle of split fuel injection was employed. The best performance obtainable with each of two different auxiliary injection systems is summarized in table II, runs 14 to 17. Spraying additional fuel downstream through six nozzles, located within the flame holder and rated at 21 gallons per hour at a differential pressure of 100 pounds per square inch, produced rough burning and no noticeable extension of the operating limits. The lean f/a limit was extended from 0.050 (run 9) to 0.032 (run 14) but the upper f/a limit was appreciably decreased when 850 pounds of fuel per hour (39 to 45 percent of total fuel flow) was sprayed 2 inches upstream of each flame-holder cluster. The additional fuel was injected

through six radial spokes manifolded outside the engine. Attached to each spoke was a modified commercial spray nozzle rated at 21 gallons per hour at 100 pounds per square inch (fig. 15). The balance of the fuel was introduced through the orifice injector. Little change in range of operation was noted when all the fuel was introduced with the auxiliary injector through nozzles rated at 55 gallons per hour (run 15).

1287

Although use of an auxiliary spray-nozzle injector lowered the lean blow-out limit, the operable f/a range was narrower than without this secondary injector. In order to extend the operable f/a range into the rich region, another auxiliary fuel injector of the orifice type, designated radial spray bars (fig. 16), was employed. Six radial 1/4-inch tubes flattened to a streamlined shape were installed 2 inches upstream of each flame-holder cluster. Each radial spray bar had a total of twelve 0.028-inch-diameter orifices, six on each side, spraying fuel in a direction normal to the air stream.

Optimum performance was obtained with an approximately constant fuel flow of 500 pounds per hour (12 to 29 percent of total fuel flow) injected at a radius of 5.38 inches through the primary orifice fuel injector and the remaining fuel injected through the auxiliary radial spray bars (runs 16 and 17). At outlet-area ratios of 0.739 and 0.676 and a p_3 of 1750 pounds per square foot absolute, the operable fuel-air ratio range was the largest of any configuration investigated. The lean limit was approximately the same as that obtained with the previously described split fuel-injection systems (about 0.030), but rich blow-out was not obtained up to the point at which the pumping capacity of the fuel system was reached (f/a = 0.098). The maximum combustion-chamber-inlet velocity attained prior to the rich pumping limit was 190 feet per second and prior to lean blow-out, 246 feet per second.

Effect of fuel-air ratio on burner performance. - The variation of combustion efficiency and total-temperature ratio with f/a for runs 9 to 11 (table II) is shown in figure 17. All data were obtained with gasoline at a combustion-chamber-inlet total temperature of 570° R and a static pressure of 1800 pounds per square foot absolute. The maximum combustion efficiencies as well as the maximum values of τ were obtained at an outlet-area ratio of 0.676 over the entire range of operation. The peak combustion efficiency of 84 percent occurred near lean blow-out, f/a of 0.05, and at a V_3 of 189 feet per second; the maximum τ of 5.8 was

reached at a f/a of 0.058 and remained constant until rich blow-out. Progressively lower values of η_b and τ were observed for outlet-area ratios of 0.739 and 0.600. At these outlet-area ratios, the change in τ between f/a of 0.059 and rich blow-out (f/a of approximately 0.070) was slight.

A comparison in terms of the fuel-air equivalence ratio E between the values of η_b and τ obtained with gasoline and kerosene at an outlet-area ratio of 0.676 is given in figure 18. Data were obtained at a combustion-chamber-inlet total temperature of 570° R for gasoline and 605° R for kerosene. The curve for gasoline was taken from figure 17 (p_3 = 1800 lb/sq ft). The kerosene data were obtained at p_3 of 1850 and 1470 pounds per square foot absolute. No significant effect of combustion-chamber pressure level on burner performance with kerosene as fuel can be observed within this pressure range.

Although the operable range of the rake burner is greater with kerosene than with gasoline, the extension is essentially in the rich region and is accompanied by a low combustion efficiency. At the same values of E, the values of η_b and τ obtained with gasoline were consistently greater than with kerosene. The combustion-chamber-inlet velocities were of the same order of magnitude for both fuels (180 to 200 ft/sec). At stoichiometric conditions, η_b was 74 percent and τ was 5.7 with gasoline and 71 percent and 5.2, respectively, with kerosene. The maximum recorded η_b with the kerosene was 78 percent and occurred at an equivalence ratio of 0.89.

The burner performance with gasoline for the split-fuel-injection configuration that resulted in the greatest extension of operating limits (runs 16 and 17, table II) is presented in figure 19. These data were taken at a T_3 of 550° R and a p_3 of 1750 pounds per square foot absolute for outlet-area ratios of 0.739 and 0.676. Approximately the same f/a operating range, η_b, and τ resulted at both outlet-area ratios. The combustion efficiency peaked with a value of 85 percent at a f/a of 0.055 and V_3 of 177 feet per second. The corresponding τ was 5.8. The value of τ increased gradually with f/a to a maximum value of 5.9 near f/a of 0.065. Further increases in f/a resulted in a slight drop in the value of τ. At an outlet-area ratio of 0.676, approximately the same combustion efficiency values were attained with or without split fuel injection (figs. 19 and 17, respectively).

At an outlet-area ratio of 0.739, however, the use of the split-fuel-injection system not only extended the operating range in both the lean and rich directions but also raised the combustion efficiency and the resulting τ several percent.

The lean blow-out occurred near a V_3 of 240 feet per second for both outlet-area ratios (table II). As previously indicated, rich blow-out could not be reached due to a limitation in the fuel-handling capacity. At the maximum f/a for which data could be taken (0.098), burning was still satisfactory. All data for the split-fuel-injection configurations were obtained at combustion-chamber-inlet velocities between 173 and 239 feet per second.

Burner Performance with Corrugated Gutter Flame Holder

Operational performance. - Best operation with the corrugated gutter flame holder (fig. 10) was obtained with the spray-nozzle injector (fig. 5) set at a radius of 5.22 inches (runs 18 to 22, table II). At an outlet-area ratio of 0.739, T_3 of 575° R, and p_3 of 1650 pounds per square foot absolute, satisfactory operation with gasoline was obtained between f/a of 0.029 and 0.059 (run 18). The V_3 varied between 206 and 279 feet per second. Reduction in outlet-area ratio to 0.676 (run 19) merely reduced the velocities to a range of 187 to 247 feet per second and caused little change in the operable f/a range.

At the larger outlet-area ratio (0.739), a reduction in the combustion-chamber-inlet static pressure from 1650 to 790 pounds per square foot absolute (run 20) shifted the operable f/a range toward slightly leaner mixtures. The corresponding combustion-chamber-inlet velocity range was 211 to 311 feet per second.

The operation of this burner was also investigated using as fuel a blend by volume of approximately 50-percent gasoline and 50-percent propylene oxide. The optimum radial fuel-injection position was identical to that for pure gasoline. At a pressure level of 1655 pounds per square foot absolute at the combustion-chamber inlet, little variation in the operable f/a range or inlet velocities from those existing with gasoline were noted (run 21). Contrary to the results obtained with pure gasoline, a reduction in p_3 from 1655 to 800 pounds per square foot absolute (run 22, table II) resulted in a slight extension of the operable f/a range.

Effect of fuel-air ratio on burner performance. - Curves of the variation in η_b and τ with fuel-air ratio for gasoline as fuel are given in figure 20. At an outlet-area ratio of 0.739, p_3 of 1650 pounds per square foot absolute, and T_3 of 575° R, data were obtained with air having a dew point of 30° F and then the same data points were repeated as closely as possible with dried air having a dew point of 2° F. For the range of dew points investigated and within the accuracy of the data, no appreciable effect of moisture content of the air on combustion efficiency was observed. It is interesting to note the accuracy with which the data points could be reproduced.

Also included in figure 20 are data for an outlet-area ratio of 0.676. As with the other two burners investigated, an outlet-area ratio of 0.739 resulted in lower combustion efficiencies and consequently lower values of τ than an outlet-area ratio of 0.676. This result is probably due to the greater combustion-chamber-inlet velocities involved at the larger nozzle-outlet areas. With the smaller outlet-area ratio, the maximum η_b of 68 percent occurred at a f/a of 0.05 and V_3 of 196 feet per second; the corresponding τ was 4.5. Although the value of η_b was slightly lowered, an increase in τ to 4.8 was achieved by increasing the f/a to 0.057.

The maximum η_b with the larger outlet-area ratio was 64 percent and occurred near rich blow-out at an f/a of 0.057 and a V_3 of 208 feet per second; the resulting τ was 4.6. At both outlet-area ratios, the general trend was for τ to increase with an increase in f/a, reaching a maximum at rich blow-out.

The effect of combustion-chamber pressure level on burner performance for the blend of 50-percent gasoline and 50-percent propylene oxide is shown in figure 21 for an outlet-area ratio of 0.739 and a total temperature of 565° R. The data were obtained at p_3 values of 1920, 1655, and 1300 pounds per square foot absolute and are plotted as a function of equivalence ratio. Only a slight variation in the operable fuel-air ratio range was observed over the range of p_3 investigated. A slight effect of pressure on the combustion efficiencies, however, was obtained. The peak combustion efficiency of 71 percent and τ of 4.8 resulted at a p_3 of 1920 pounds per square foot absolute near the rich blow-out condition ($E = 0.8$). Below rich blow-out, greater η_b resulted at a pressure level of 1300 than at either 1655 or 1920 pounds per

square foot absolute. This unexpected reverse effect of p_3 on η_b may be partly due to changes in fuel pressure and the resulting fuel distribution. The fuel-pressure range for each value of p_3 level is therefore given on the figure. Inasmuch as the maximum spread in η_b for the three pressure levels was small, a single curve for τ was drawn through all the data. The value of τ increased almost linearly with equivalence ratio and the combustion-chamber-inlet velocities ranged from 200 to 270 feet per second.

A direct comparison can be made at a p_3 of approximately 1650 pounds per square foot absolute of the burner performance with gasoline (fig. 20) and with blended fuel (fig. 21). At the same fuel-air equivalence ratio, the combustion efficiencies and total-temperature ratios obtained with the blend were a few percent above those obtained with the gasoline. Because the operable range with pure gasoline was greater than with the blend, the maximum τ obtained with the gasoline (4.7 at $E = 0.85$) was greater than that obtained with the blend (4.2 at $E = 0.70$).

A comparison of the performance obtained with the two fuels at p_3 of 800 pounds per square foot absolute is made in figure 22. Burner performance is again presented as a function of fuel-air equivalence ratio at an outlet-area ratio of 0.739 and T_3 of 565° and 580° R. At this low combustion-chamber pressure level, a pressure ratio at the nozzle outlet sufficient for choking could not be obtained; however, an approximately constant pressure ratio was maintained across the engine. The rich and lean limits occurred at about a fuel-air equivalence ratio of 0.35 and of 0.75, respectively, for both fuels. At this combustion-chamber pressure level, the blend was superior to the gasoline only at the leaner conditions; essentially the same η_b and τ values could be obtained at a given E in the richer regions with either fuel. For both fuels, η_b and consequently τ increased sharply with fuel-air equivalence ratio and reached a maximum of 79 percent and 5.0, respectively, at an E of 0.76 for gasoline and 75 percent and 4.8 at E of 0.73 for the blended fuel. The range of V_3 at this low p_3 was from 196 to 311 feet per second and corresponded to combustion-chamber-inlet Mach number M_3 values between 0.168 and 0.262.

The trend established in figure 21 of the combustion efficiencies with the blend being greater at a reduced combustion-chamber pressure level (1300 lb/sq ft absolute) than at the higher

pressures is further illustrated at 800 pounds per square foot absolute in figure 22. A similar trend of the combustion efficiency rising with a decrease in the combustion-chamber pressure level from 1650 to 800 pounds per square foot absolute was exhibited with pure gasoline (figs. 20 and 22). The reduction in pressure level was also accompanied by a slight shift in the operable fuel-air equivalence-ratio range toward the lean region. The peak η_b was only 64 percent and the peak T was 4.6 at p_3 of 1650 pounds per square foot absolute and occurred at E of 0.86 (fig. 20); whereas at p_3 of 800 pounds per square foot absolute, the peak η_b was 79 percent and the peak T was 5.0 and occurred at a leaner mixture E of 0.76 (fig. 22). The inlet temperatures and velocities at both pressure levels were similar. The reasons for these unexpected variations in burner performance with pressure level are not fully understood. Other variables in addition to combustion-chamber-inlet pressure were probably involved and these unknown variables have not been included in the data evaluation.

Combustion-Chamber Pressure Recovery

Representative total-pressure ratios P_6/P_3 across the combustion chamber for the rake and corrugated gutter burners are presented as a function of T in figure 23 for outlet-area ratios of 0.739 and 0.676. The pressure ratios for the serrated annular baffle burner are similar to those obtained with the rake burner and are therefore not shown.

The pressure losses across the combustion chamber arise from the addition of heat to a flowing gas and from the frictional losses of the flame holder and the combustion chamber. The pressure loss due to the addition of heat is primarily a function of M_3 and T, whereas the frictional losses depend primarily on M_3 (reference 7). For a given burner and at a fixed outlet-area ratio, the two losses combine to give a relatively small change in pressure ratio over the entire range of T. For example, between T values of 4 and 6 and at M_3 values ranging from 0.16 to 0.21, the pressure ratio across the combustion chamber at a given outlet-area ratio (0.739) varied only 0.015 with the rake burner. At a lower range of T, values obtained with the corrugated gutter burner at the same outlet-area ratio and for M_3 values between 0.18 and 0.23, the total change in the pressure ratio was only 0.05.

This slight change in the pressure ratio across the combustion chamber over the entire operating range of a given configuration facilitates the analytical treatment of over-all ram-jet performance by permitting the use of an assumed constant combustion-chamber pressure loss.

The variation in total-pressure ratio across the combustion chamber over the entire operating range of all configurations presented in figure 23 is only 0.76 to 0.88. The larger losses occur at the low values of τ, because under such a condition the high values of M_3 are encountered.

SUMMARY OF RESULTS

The combustion performance of a 16-inch ram jet with each of three burner configurations (rake, serrated annular baffle, and corrugated gutter burners) was determined in the Lewis altitude wind tunnel under controlled conditions of combustion-chamber-inlet pressure and temperature, fuel flow, and nozzle-outlet area. The results obtained are summarized as follows:

1. A different optimum fuel-injection radius usually existed for each combination of burner and fuel. A change of as little as 1/4-inch from the optimum position could cause a serious reduction in combustion efficiency, rough and unsteady burning, and in some instances blow-out.

2. Based on the values of combustion efficiency and total-temperature ratio obtained, gasoline proved a superior fuel to kerosene for both the rake and the annular baffle burner configurations. Data obtained with the corrugated gutter burner indicated that a blend of 50-percent gasoline and 50-percent propylene oxide might have characteristics slightly superior to pure gasoline.

3. Because of the magnitude of the combustion-chamber-inlet Mach numbers, an equal and sometimes slightly greater combustion-chamber pressure drop was experienced at the lean fuel-air ratios and the low total-temperature ratios than at the richer mixtures and high total-temperature ratios with all burner configurations investigated.

4. For all burners, greater combustion efficiency and total-temperature ratio were obtained at an outlet-area ratio of 0.676 than at 0.739, the maximum value investigated.

[redacted]

5. No effect on burner performance over a combustion-air dew point range of 2° to 30° F was apparent.

6. The maximum combustion efficiency obtained with the serrated annular baffle burner was 82 percent at a fuel-air ratio of 0.054 and a combustion-chamber-inlet velocity of 180 feet per second. The corresponding total-temperature ratio was 5.7. The maximum total-temperature ratio attained was 6.0. Lean blow-out was estimated to occur for each of the three outlet-area ratios investigated at a combustion-chamber-inlet velocity of approximately 200 feet per second. The operational performance of the burner was sensitive to a reduction in the combustion-chamber pressure level from 1750 to 1365 pounds per square foot absolute.

7. The maximum fuel-air ratio operating range of 0.030 to 0.098 (upper limit imposed by fuel-pumping capacity) resulted when a split-injection-fuel system was employed with the rake burner. A maximum combustion efficiency of 85 percent was also obtained with this configuration at a fuel-air ratio of 0.055 and a total-temperature ratio of 5.8. All data obtained were for combustion-chamber-inlet velocities between 173 and 239 feet per second.

8. The best performance at low combustion-chamber pressure level was obtained with the corrugated gutter burner. Noticeably higher combustion efficiencies and total-temperature ratios were observed at 800 than at 1920 pounds per square foot absolute at the combustion-chamber inlet. The maximum combustion efficiency of 79 percent occurred at a combustion-chamber-inlet pressure of 800 pounds per square foot absolute. Other variables in addition to combustion-chamber-inlet pressure were probably involved and these unknown variables have not been included in the data evaluation. The range of combustion-chamber-inlet velocities over which this burner was investigated was 188 to 311 feet per second.

Lewis Flight Propulsion Laboratory,
National Advisory Committee for Aeronautics,
Cleveland, Ohio.

REFERENCES

1. Connors, James F., and Schroeder, Albert H.: Experimental Investigation of Pressure Fluctuations in 3.6-Inch Ram Jet at Mach Number 1.92. NACA RM E9H12, 1949.

2. Dailey, C. L.: Comments on the Subcritical Buzz Phenomenon Encountered with Supersonic Ramjet Diffusers. Rep. 5-1-16, Aero. Lab., USCAL, June 1, 1948. (Navy Contract NOa(s)9242.)

3. Messing, Wesley E., and Simpkinson, Scott H.: Free-Flight Performance of 16-Inch-Diameter Supersonic Ram-Jet Units. II - Five Units Designed for Combustion-Chamber-Inlet Mach Number of 0.16 at Free-Stream Mach Number of 1.60 (Units B-1, B-2, B-3, B-4, and B-5). NACA RM E50B14, 1950.

4. Sterbentz, William H., and Wilcox, Fred A.: Investigation of Effects of Movable Exhaust-Nozzle Plug on Operational Performance of 20-Inch Ram Jet. NACA RM E8D22, 1948.

5. Wilcox, Fred A., and Howard, Ephraim M.: Comparison of Two Fuels in Bumblebee 18-Inch Ram Jet Incorporating Rake-Type Flame Holder. NACA RM E8F11, 1948.

6. Howard, Ephraim M., Wilcox, Fred A., and Dupree, David T.: Combustion-Chamber Performance with Four Fuels in Bumblebee 18-Inch Ram Jet Incorporating Various Rake- or Gutter-Type Flame Holders. NACA RM E8I01a, 1948.

7. Sterbentz, William H.: Analysis and Experimental Observation of Pressure Losses in Ram-Jet Combustion Chambers. NACA RM E9H19, 1949.

8. Perchonok, Eugene, Wilcox, Fred A., and Sterbentz, William H.: Preliminary Development and Performance Investigation of a 20-Inch Steady-Flow Ram Jet. NACA ACR E6D05, 1946.

9. Perchonok, Eugene, Sterbentz, William H., and Wilcox, Fred A.: Performance of a 20-Inch Steady-Flow Ram Jet at High Altitudes and Ram-Pressure Ratios. NACA RM E6L06, 1947.

TABLE I - TABLE OF COORDINATES FOR 16-INCH RAM JET

Distance from supersonic-diffuser inlet (in.)	Diameter of inner body (in.)	Diameter of outer body (in.)	Remarks
0	----	----	Inlet to supersonic diffuser (free-jet investigation only)
6	4.2	9.92	Subsonic-diffuser inlet (corresponds to station 2, fig. 2)
12	4.74	10.56	Front center-body support (station y, fig. 2)
24	5.56	11.80	
36	6.28	13.04	
48	6.96	14.30	
62	7.86	15.80	Air-flow measuring station (station x, fig. 2)
65	8.00	16.00	
74	8.00	16.00	Fuel-injector location
80.7	7.25	16.00	Pilot burner
91	6.00	16.00	Combustion-chamber inlet (station 3, fig. 2)
92	0	16.00	
172	Variable	16.00	Nozzle inlet (station 5, fig. 2)
181	Variable	13.75	Engine outlet (station 6, fig. 2)

[redacted]

[redacted]

TABLE II - SUMMARY OF CONFIGURATIONS INVESTIGATED AND RESULTS OBTAINED

Run	Flame holder	Fuel injector	Fuel-injection radius (in.)	Outlet-area ratio A_6/A_4	Combustion-chamber inlet: Static pressure p_3 (lb/sq ft abs.)	Combustion-chamber inlet: Total temperature T_3 (°R)	Fuel-air ratio, f/a (a)	Fuel	Figure
1	Annular	Orifice	5.22	0.739	1750 ±20	540 ±20	V_3 = 195 O–I–O 194	Gasoline	13
2			5.22	.676	1750 ±20	540 ±20	204 O–I–O 174	Gasoline	13
3			5.22	.600	1750 ±20	540 ±20	196 O–I–O 156	Gasoline	13
4			5.22	.600	1565 ±5	540 ±20	177 O–I–O 157	Gasoline	13
5			5.38	.676	1800 ±5	540 ±20	193 I–I 191	Gasoline	--
6			5.94	.739	1790 ±15	555 ±10	191 O–I–● 169	Kerosene	14
7			5.94	.676	1790 ±15	555 ±10	176 O–I–● 176	Kerosene	14
8			5.94	.600	1790 ±15	555 ±10	174 O–I–● 161	Kerosene	14
9	Rake	Orifice	5.94	0.739	1800 ±7	570 ±10	206 O–I–O 195	Gasoline	17
10		Orifice	5.94	.676	1800 ±7	570 ±10	190 O–I–O 179	Gasoline	17
11		Orifice	5.94	.600	1800 ±7	570 ±10	180 O–I–O 165	Gasoline	17
12		Orifice	5.74	.676	1470 ±10	605 ±10	204 O–I–▷ 190	Kerosene	18
13		Orifice	5.74	.676	1850 ±10	606 ±10		Kerosene	18
14		Orifice	5.74	.600	1850 ±10	606 ±10	185 O–I–▷ 169	Kerosene	--
15		Orifice and spoke with spray nozzle[c]	5.94	.739	1710 ±90	560 ±5	242 O–I–O 206	Gasoline	--
16		Spoke with spray nozzle[d]		.739	1790 ±5	555 ±5	244 O–I–O 205	Gasoline	--
17		Orifice and radial spray bar	5.38	.739	1750 ±10	560 ±10	246 O–I–▷ 190	Gasoline	19
		Orifice and radial spray bar	5.38	.676	1750 ±10	560 ±10	236 O–I–▷ 173	Gasoline	19
18	Corrugated gutter	Spray nozzle	5.22	0.739	1650 ±15	575 ±10	279 O–I–O 206	Gasoline	20
19			5.22	.676	1650 ±15	575 ±10	247 O–I–O 187	Gasoline	20
[e]20			5.22	.739	790 ±20	580 ±5	311 ●–I–● 211	Gasoline	22
21			5.22	.739	1655 ±10	565 ±5	283 O–I–O 207	Propylene oxide, 50 percent; gasoline, 50 percent	21
[e]22			5.22	.739	800 ±10	565 ±5	298 O–I–● 196	Propylene oxide, 50 percent; gasoline, 50 percent	22

Fuel-air ratio, f/a (a): .03 .04 .05 .06 .07 .08 .09 .10

[a]Data point before blow-out, I; blow-out point, O; estimated combustion-chamber-inlet velocity, V_3, ft/sec.

[b]Limitations of equipment prohibited higher fuel-air ratio.

[c]Rated at 21 gal/hr at 100 lb/sq in.

[d]Rated at 55 gal/hr at 100 lb/sq in.

[e]Outlet not choked.

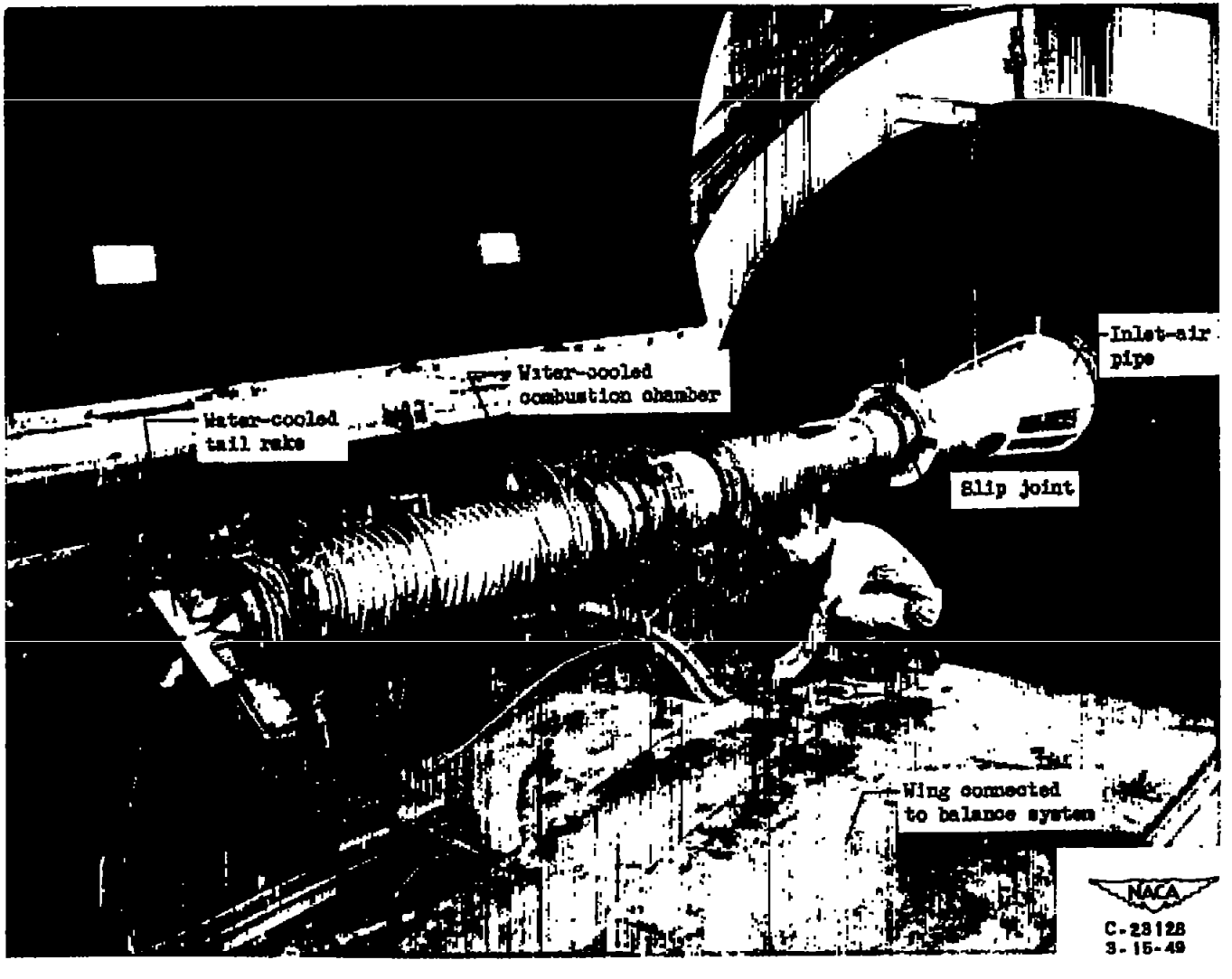

Figure 1. - Connected-pipe installation of 16-inch ram jet in altitude wind tunnel.

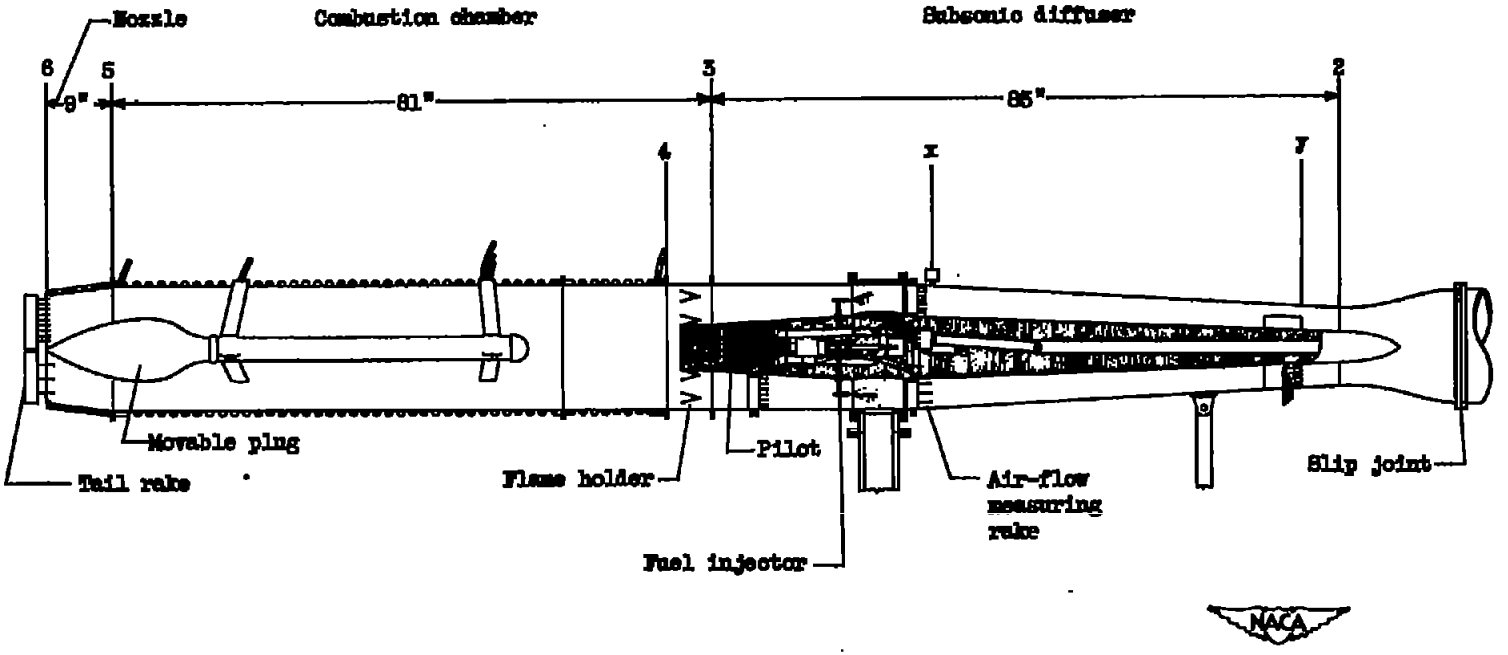

Figure 2. - Schematic diagram of 16-inch ram jet.

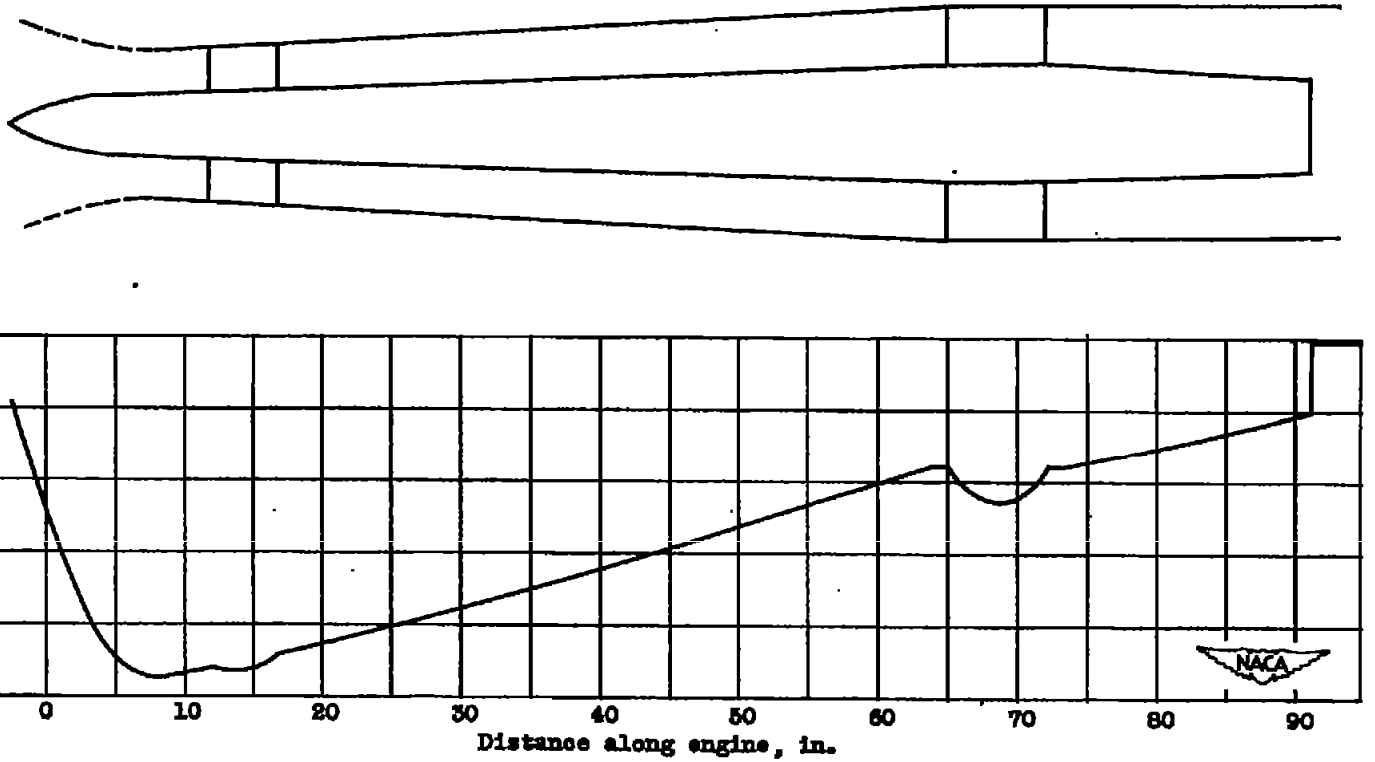

Figure 3. - Variation of flow area through ram-jet diffuser.

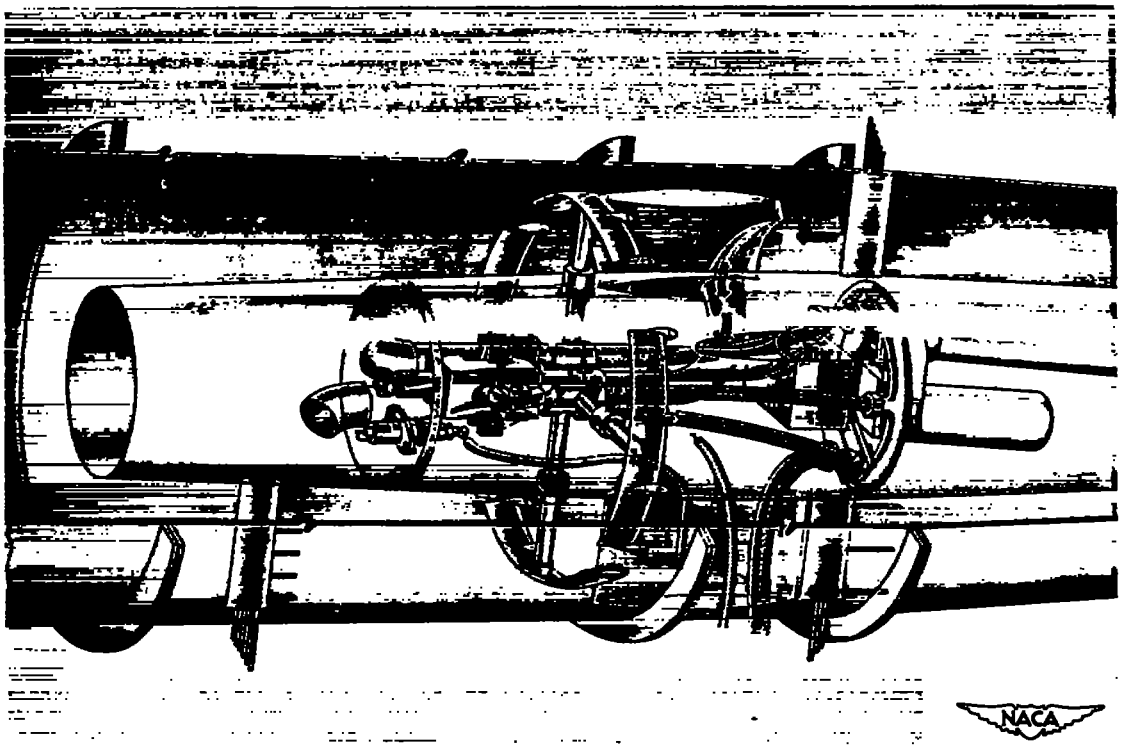

Figure 4. - Vortex pilot and fuel-injector details.

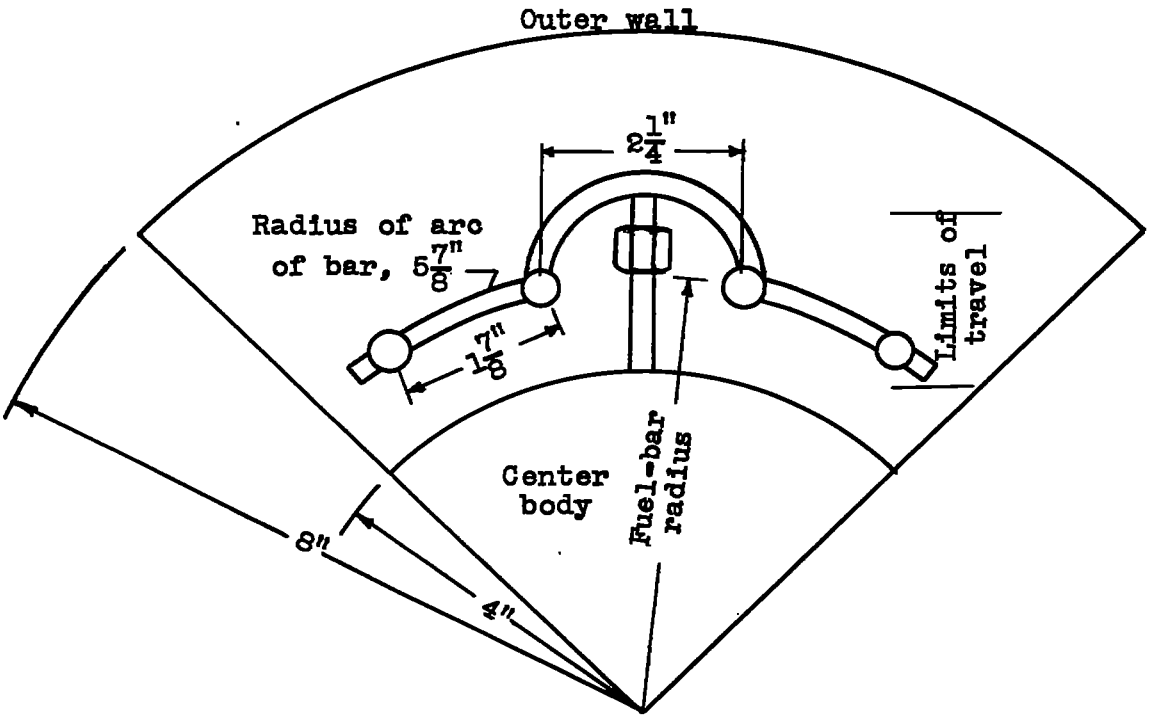

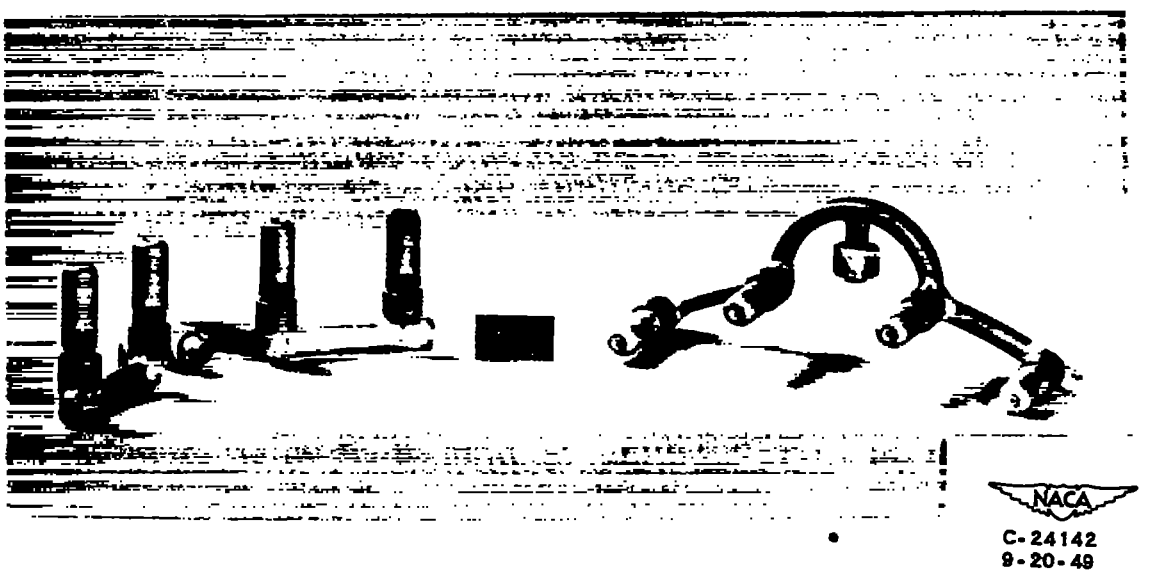

Figure 5. - Spray-nozzle fuel injector.

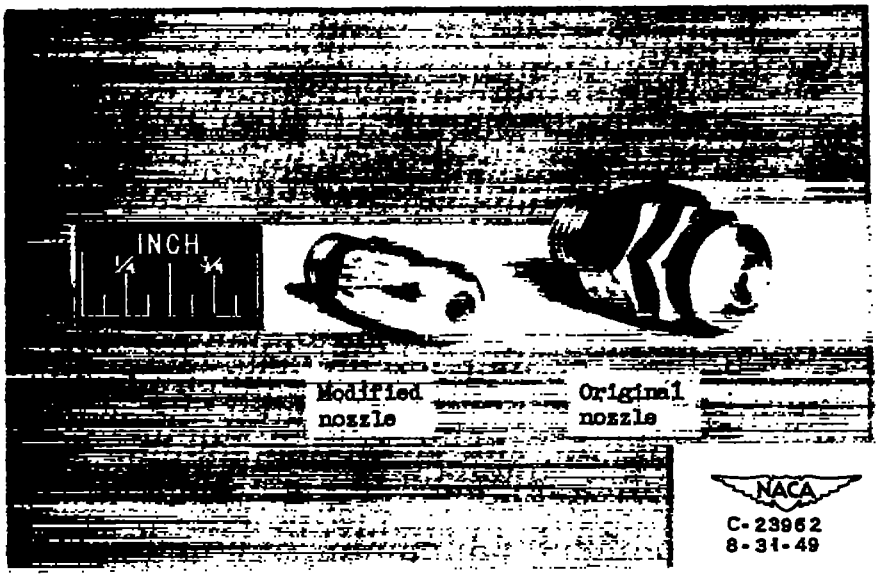

Figure 6. - Externally modified and original fuel-injection nozzles.

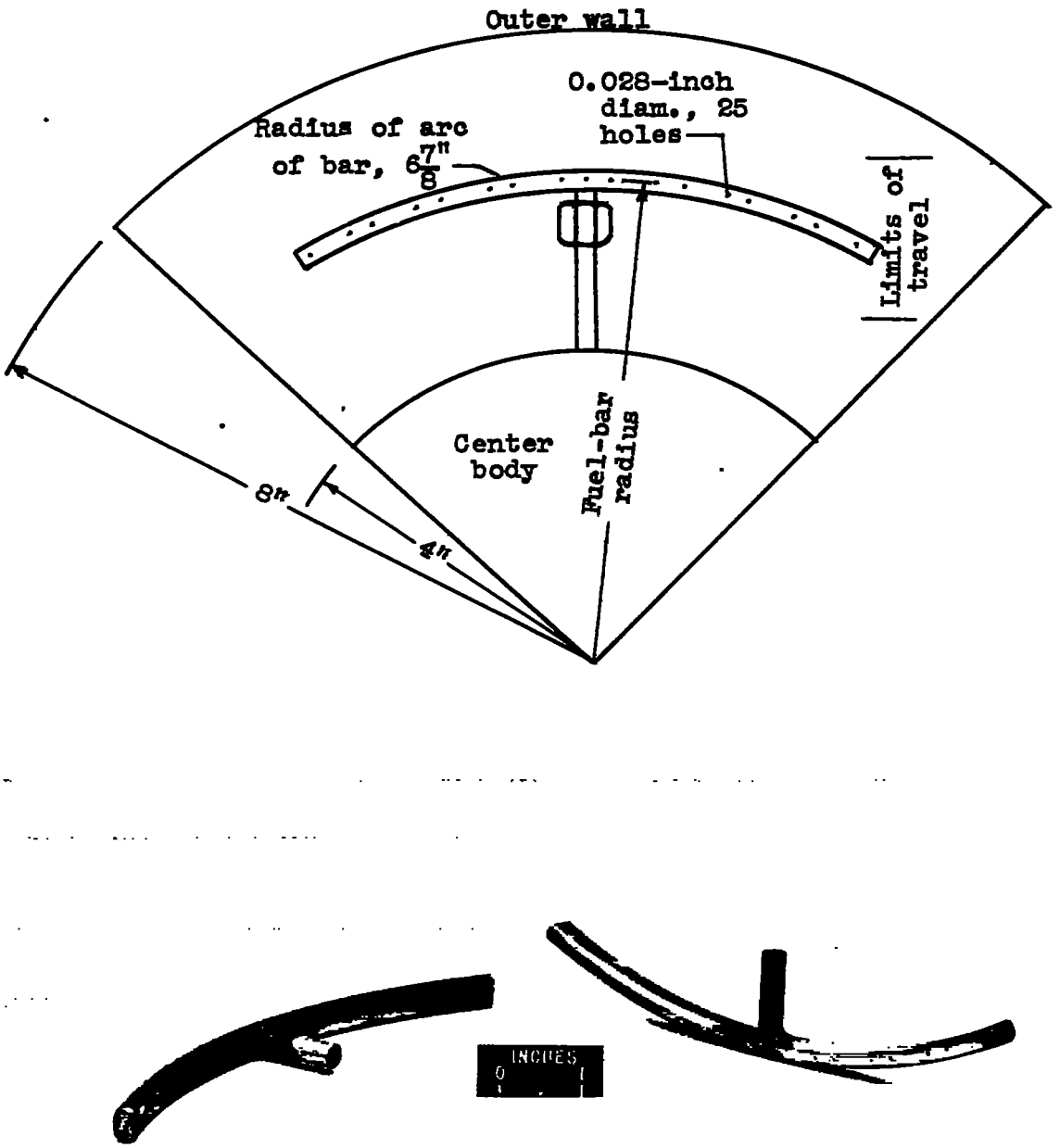

Figure 7. - Orifice fuel injector.

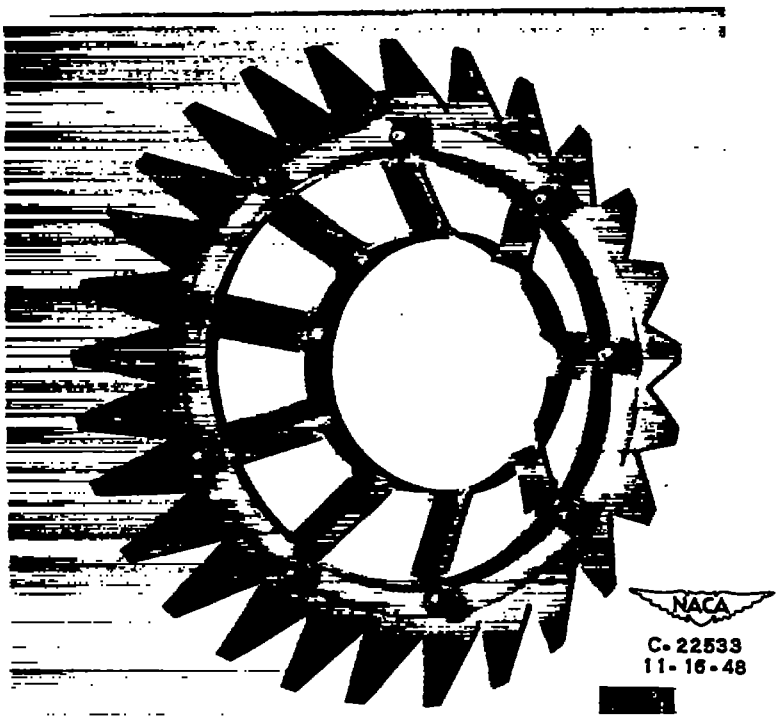

(a) Downstream view.

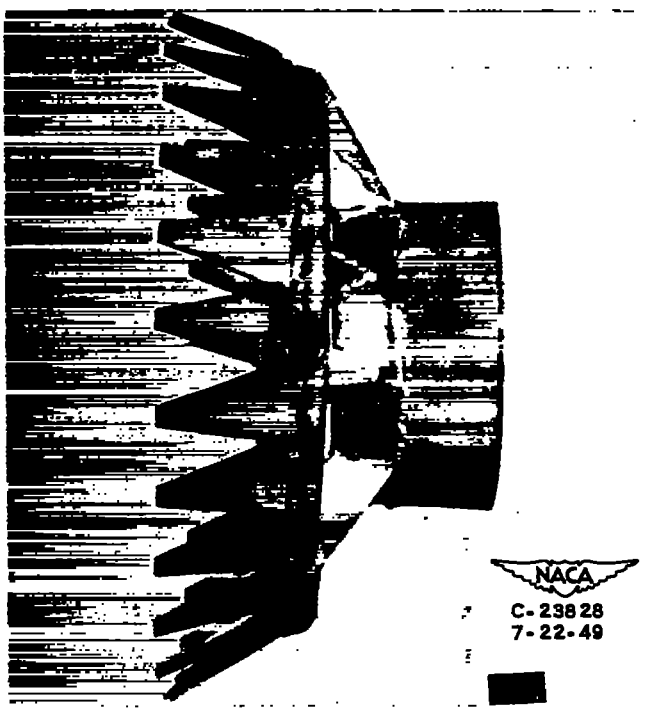

(b) Side view.

Figure 8. - Serrated annular baffle flame holder.

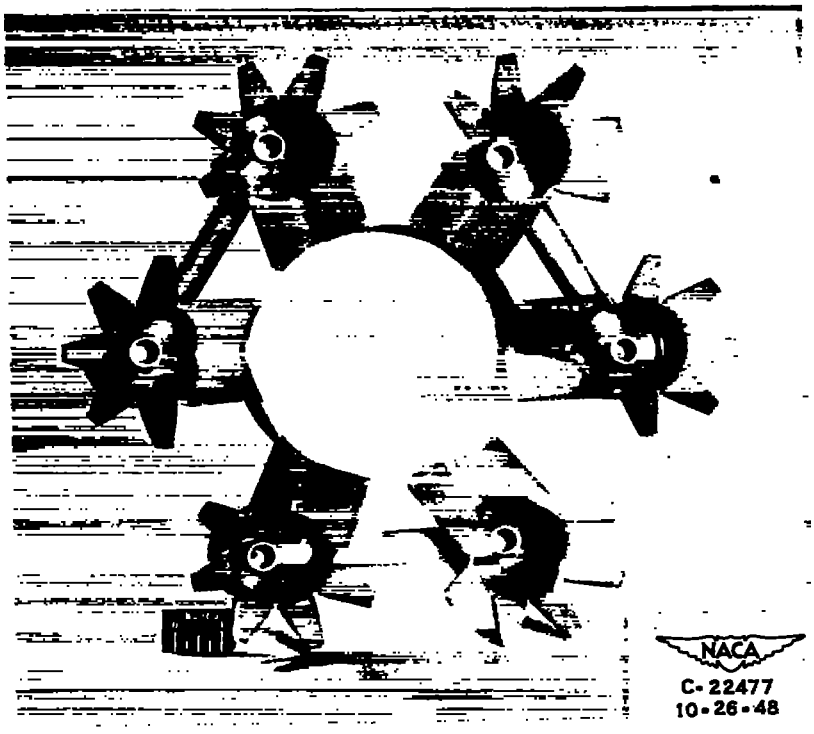

(a) Downstream view.

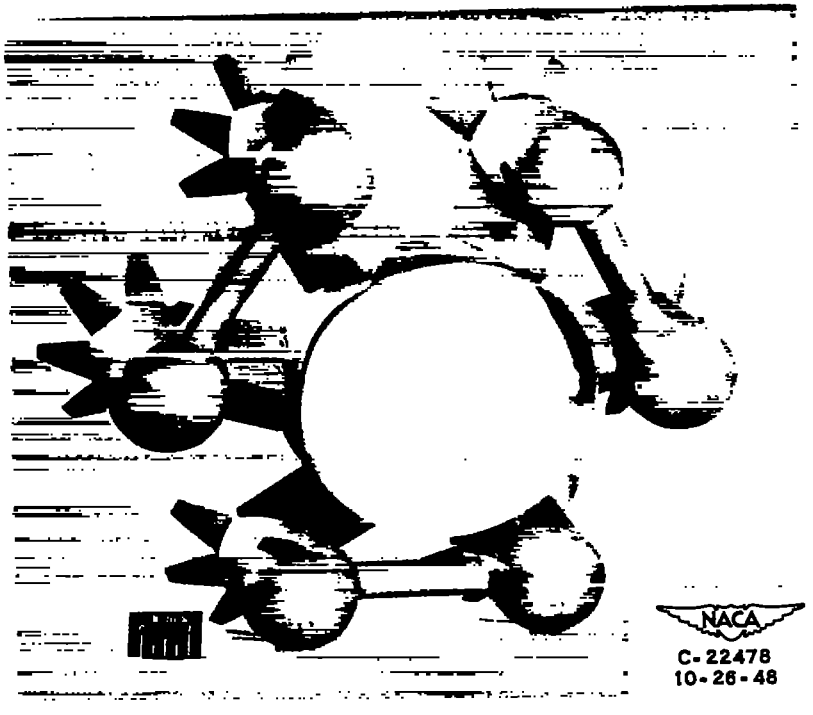

(b) Upstream view.

Figure 9. - Rake flame holder.

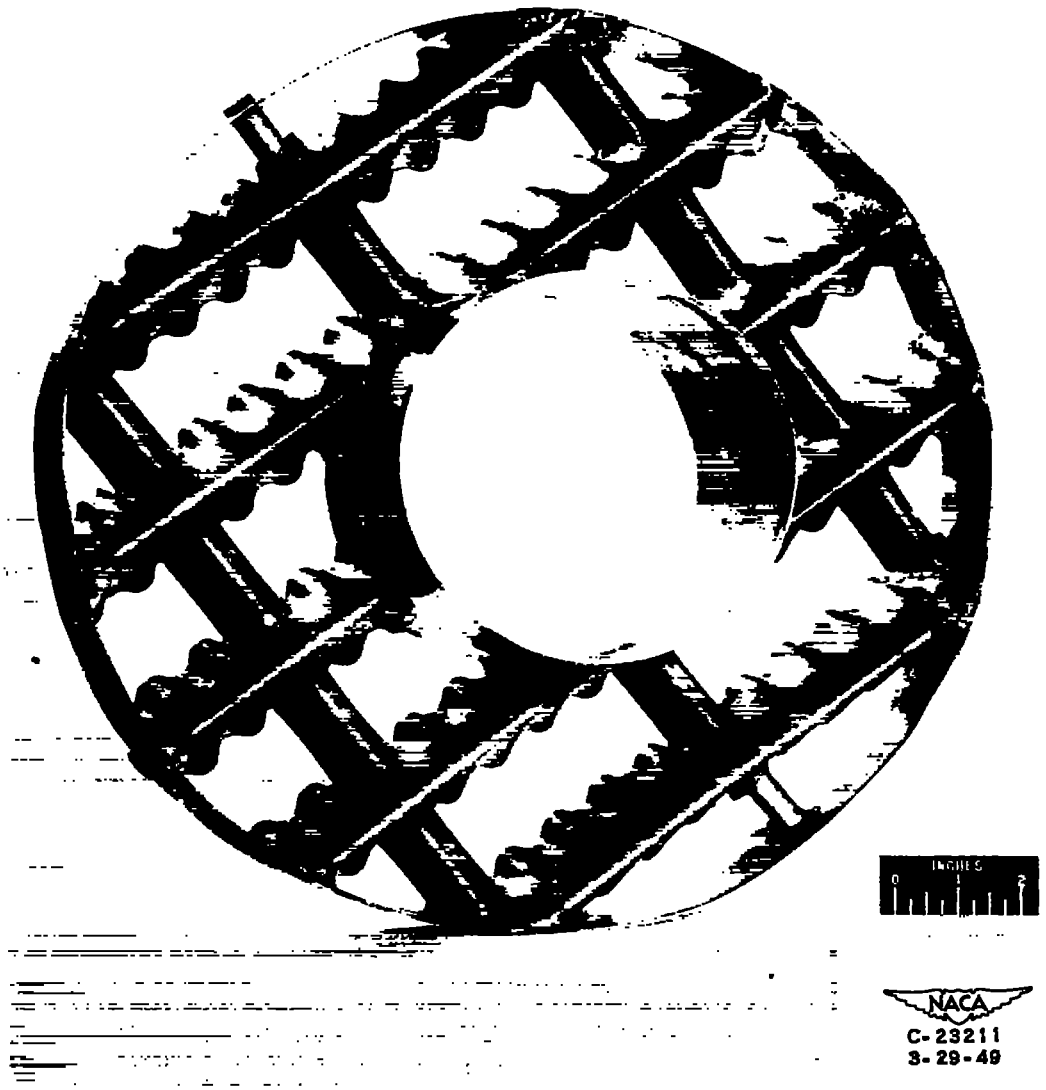

Figure 10. - Upstream view of corrugated gutter flame holder.

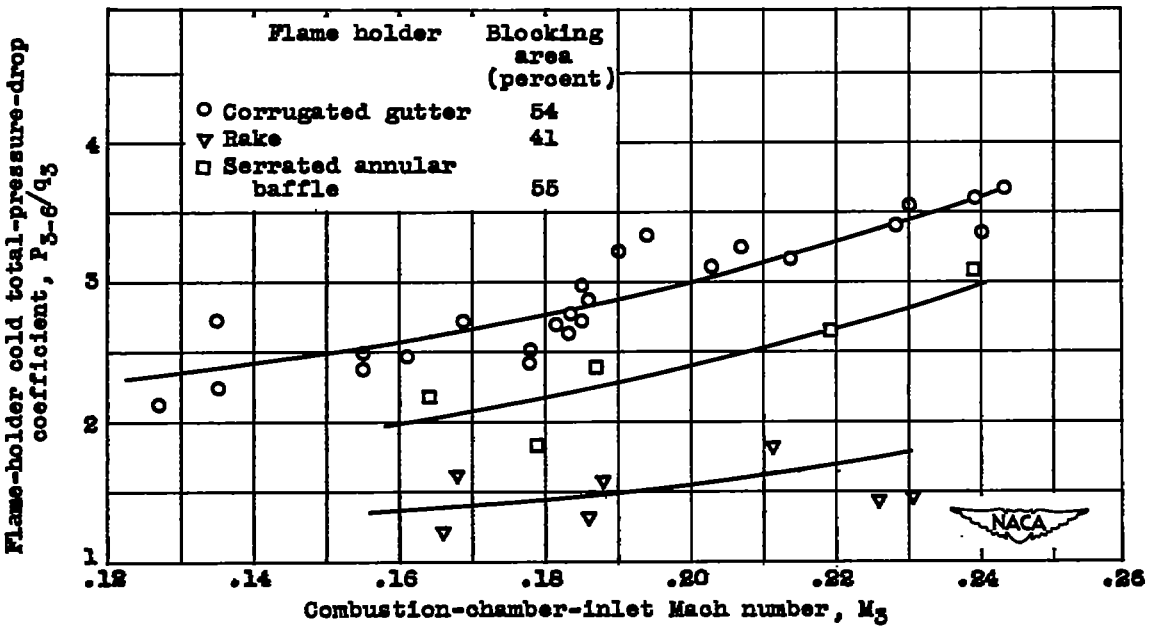

Figure 11. - Comparison of pressure-loss characteristics of three flame holders investigated.

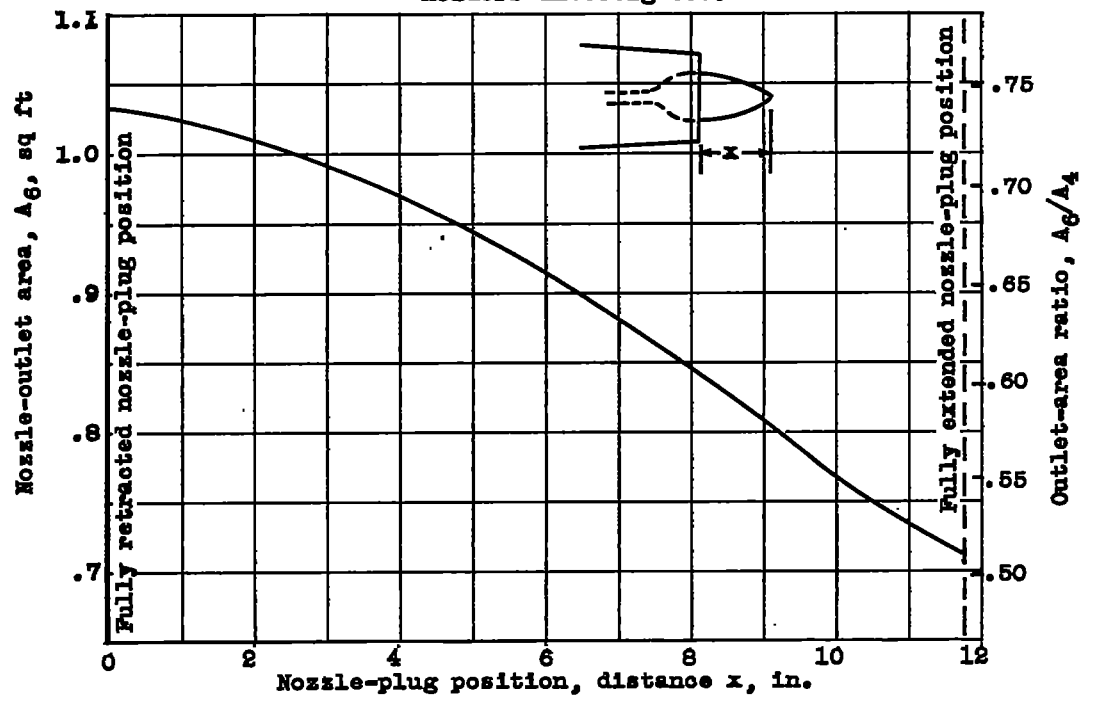

Figure 12. - Effect of nozzle-plug position on nozzle-outlet area.

[redacted]

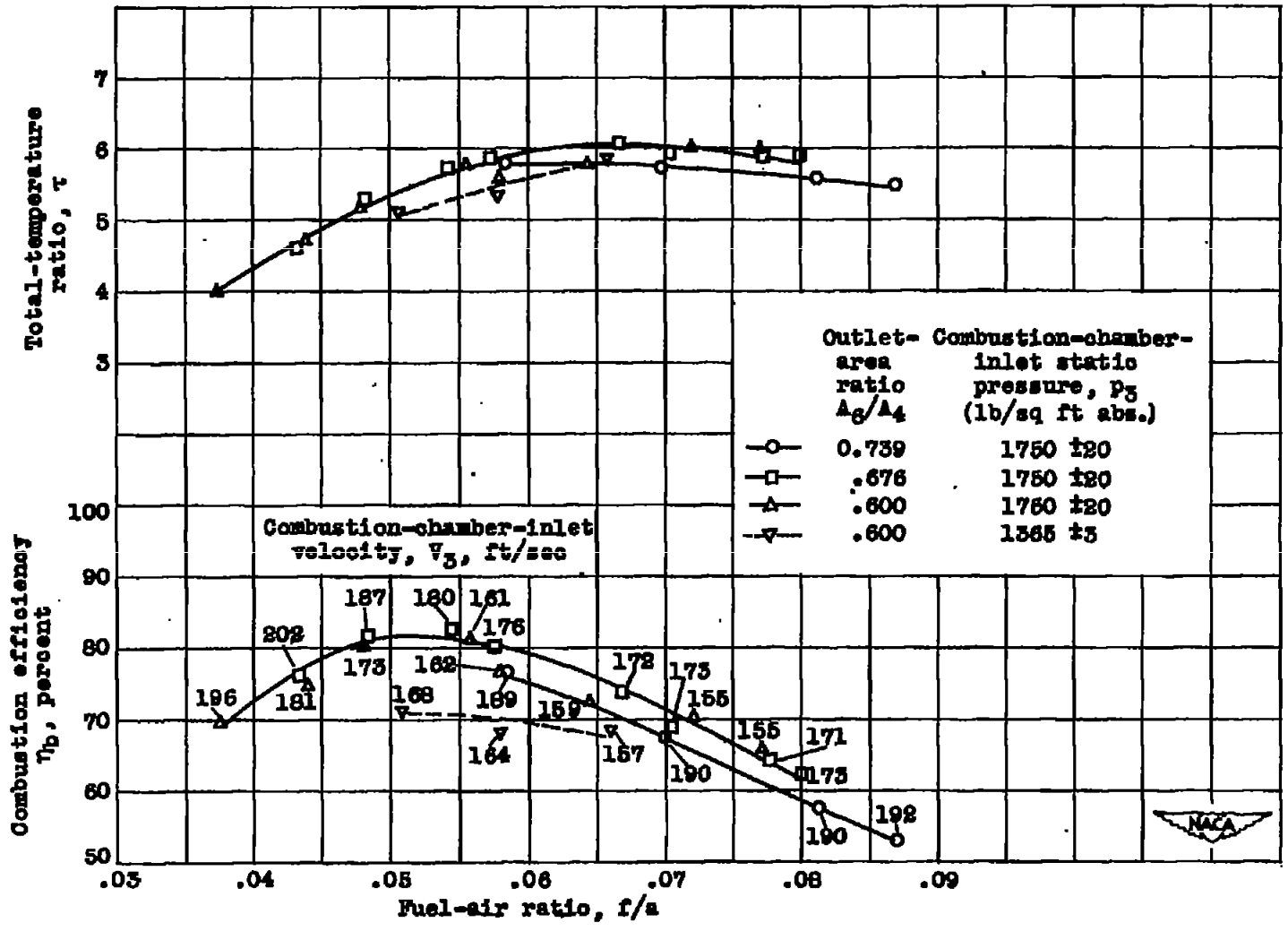

Figure 13. - Effect of fuel-air ratio on combustion efficiency and total-temperature ratio across combustion chamber with serrated annular baffle burner. Fuel, gasoline; combustion-chamber-inlet total temperature, 540° ±20° R.

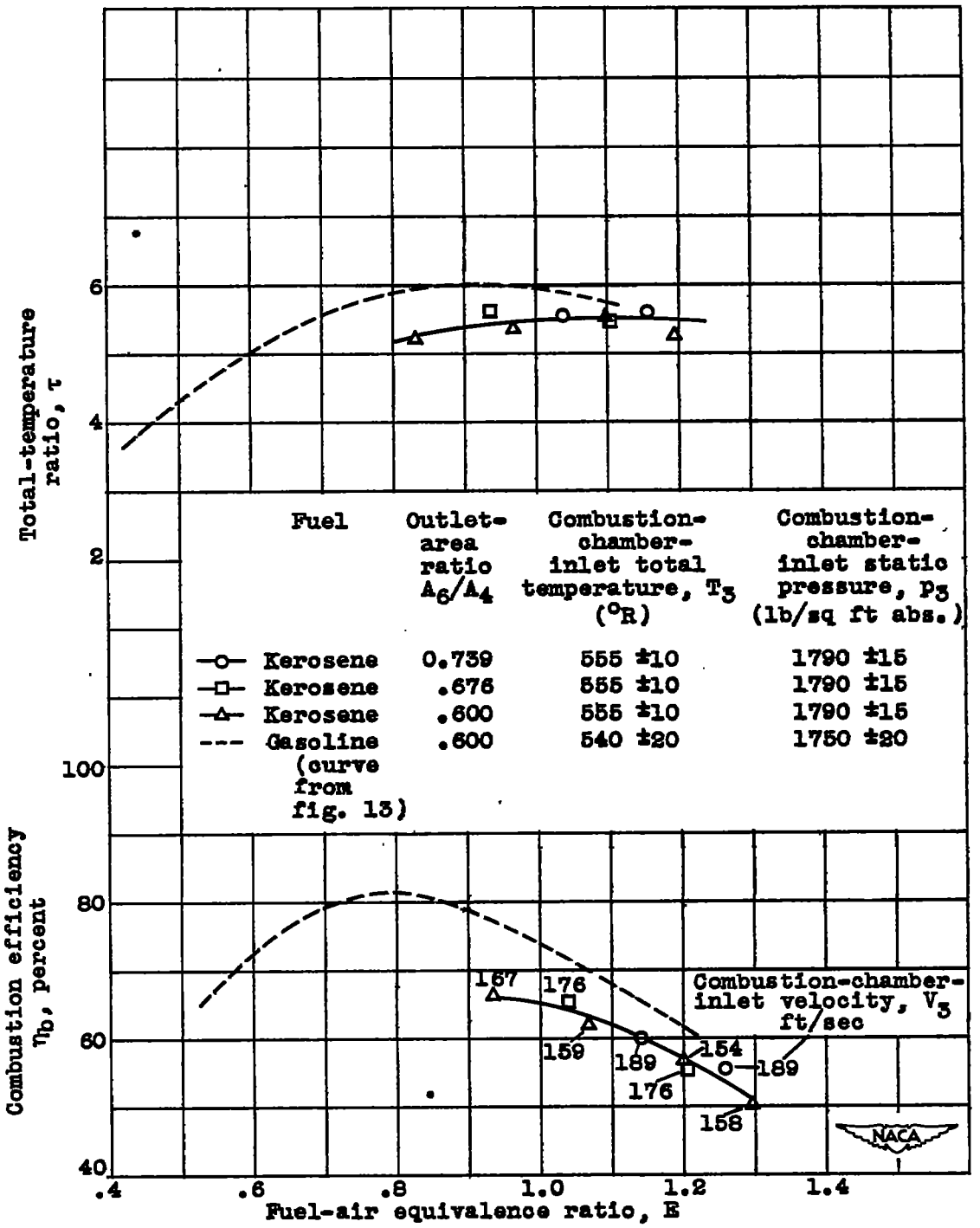

Figure 14. - Comparison of combustion performance of serrated annular baffle burner with gasoline or kerosene as fuel.

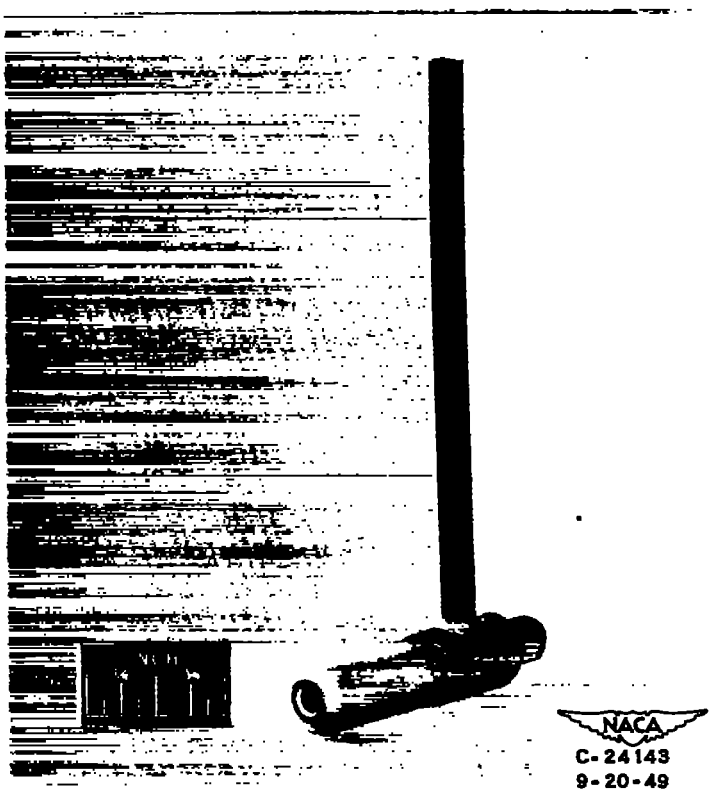

Figure 15. - Auxiliary fuel injector consisting of spoke and modified commercial spray nozzle.

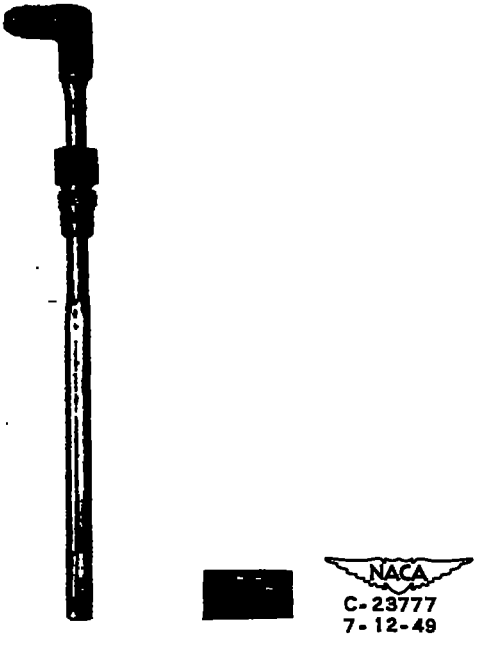

Figure 16. - Auxiliary fuel injector consisting of spoke and orifice-type radial spray bar.

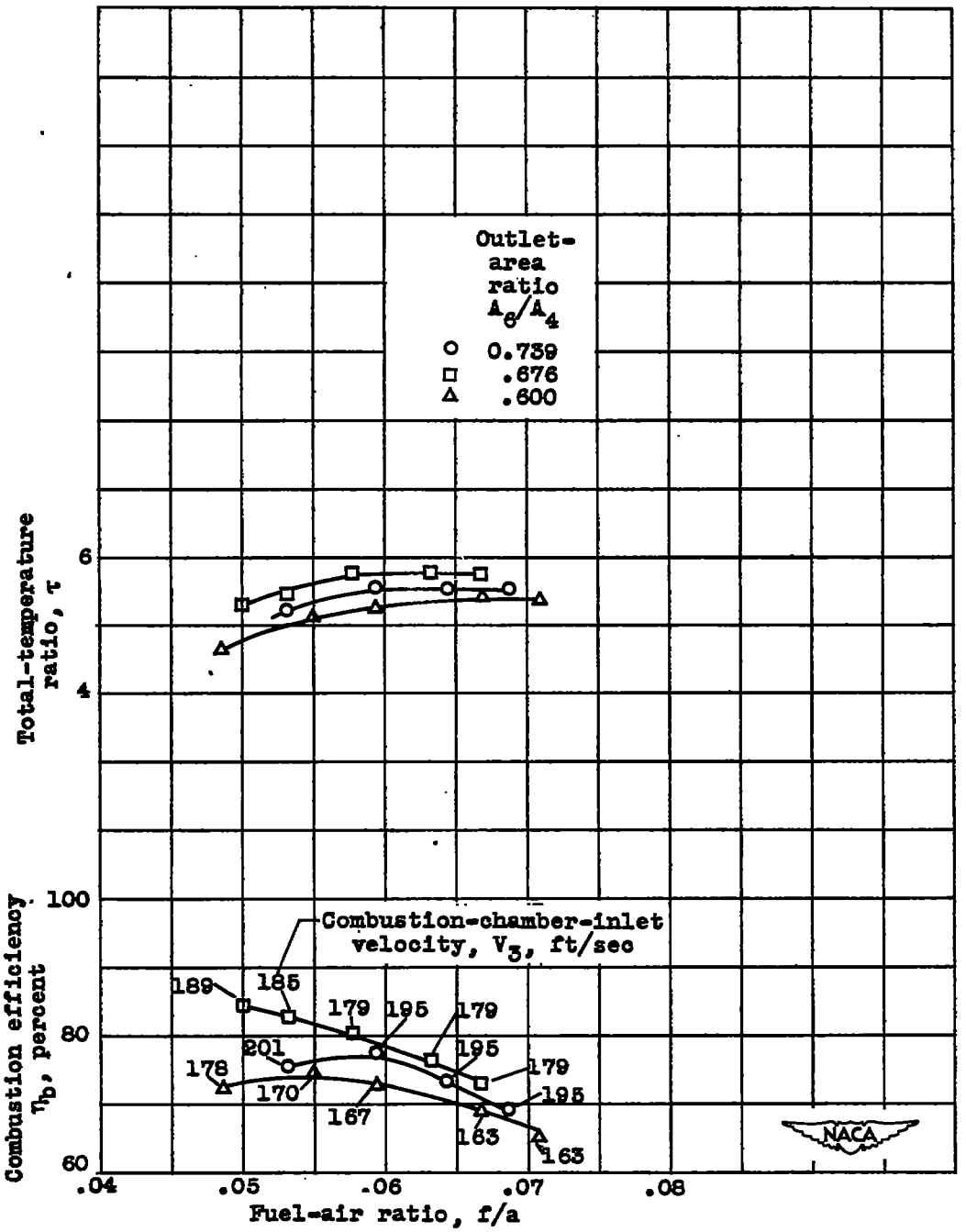

Figure 17. - Effect of fuel-air ratio on combustion efficiency and total-temperature ratio across combustion chamber. Rake burner; fuel, gasoline; combustion-chamber-inlet static pressure, 1800 ±7 pounds per square foot absolute; combustion-chamber-inlet total temperature, 570° ±10° R.

[redacted]

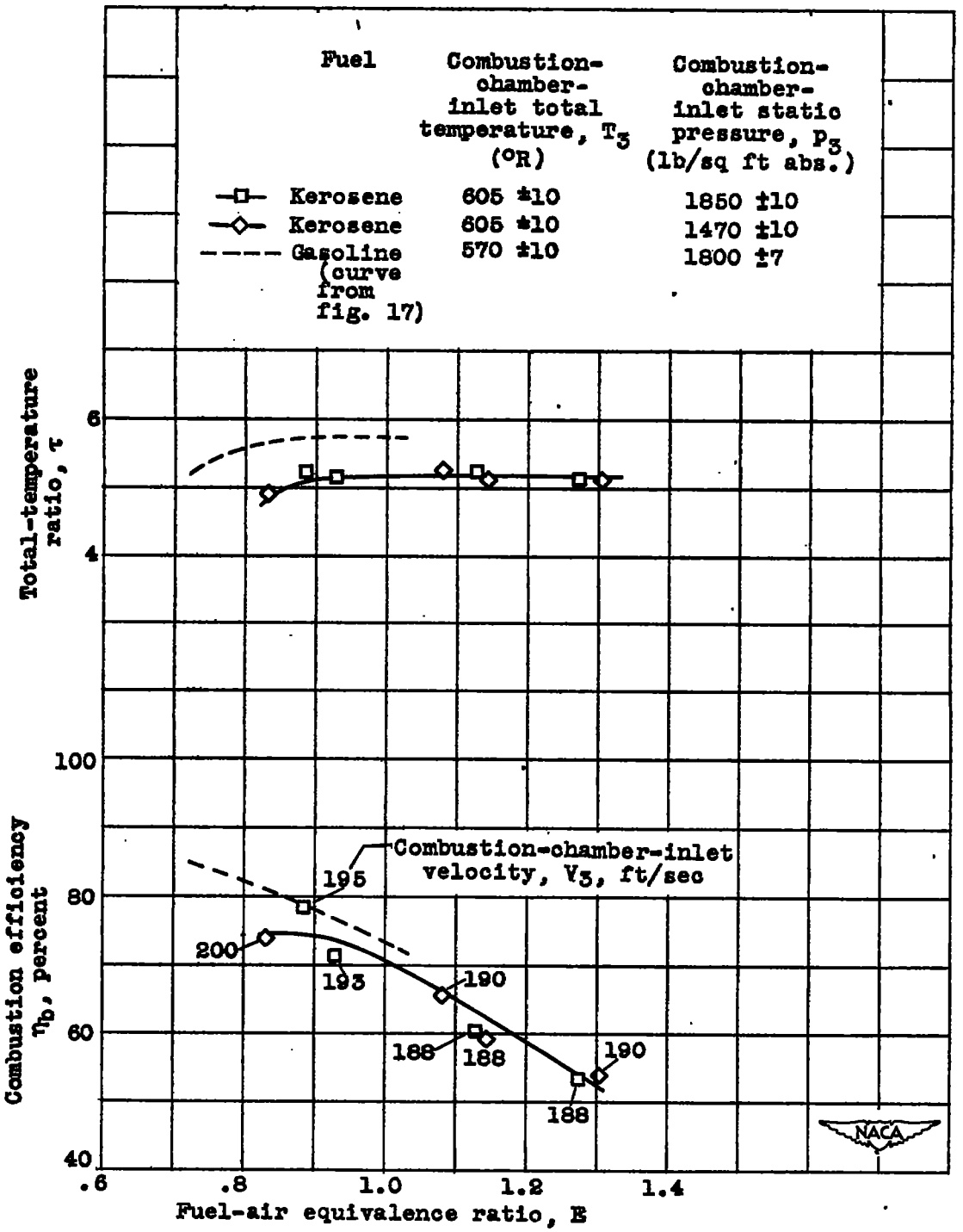

Figure 18. - Comparison of combustion performance of rake burner with gasoline or kerosene as fuel. Outlet-area ratio, 0.676.

[redacted]

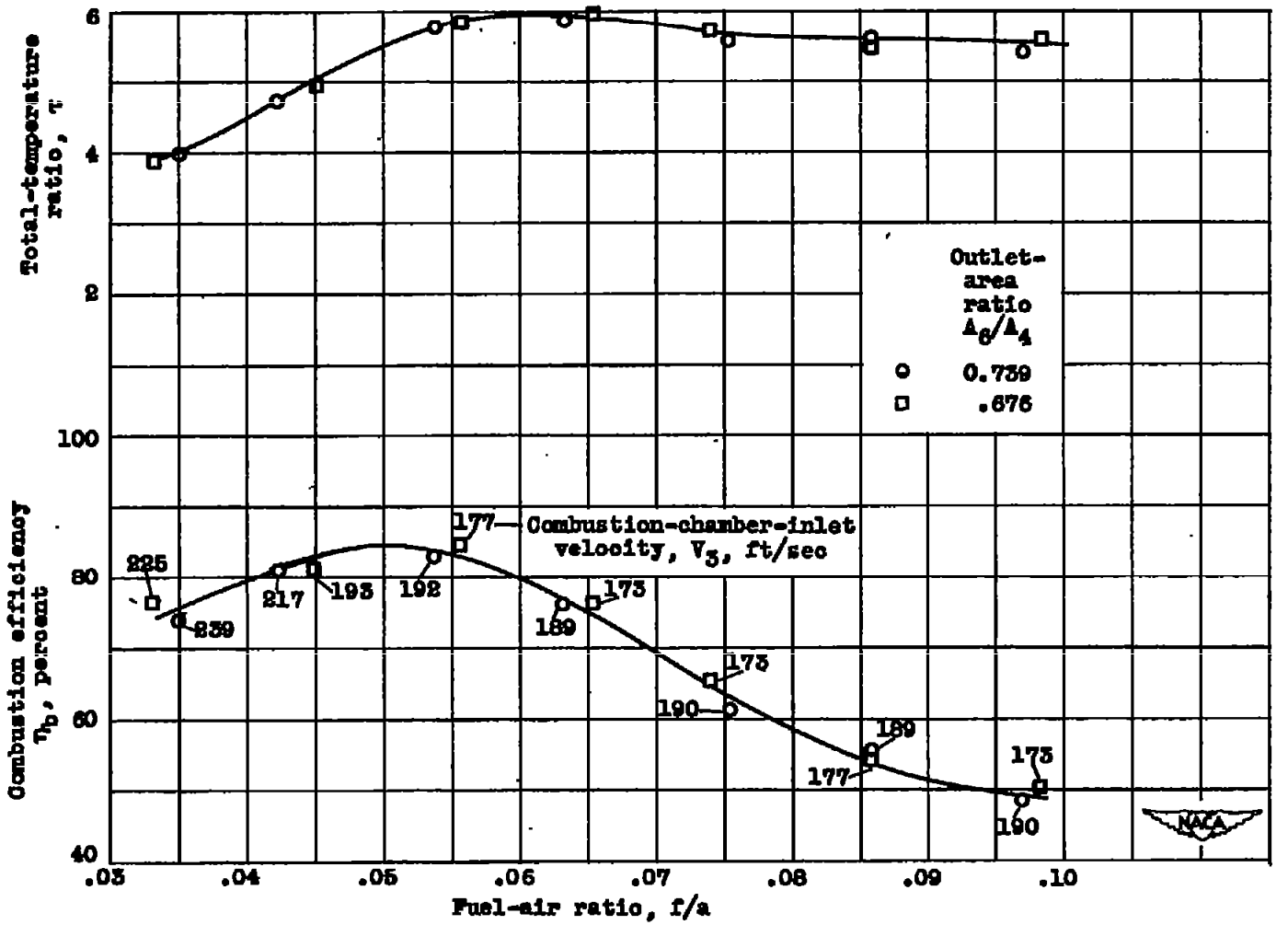

Figure 19. - Effect of fuel-air ratio on combustion efficiency and total-temperature ratio across combustion chamber with rake burner and radial-spray-bar auxiliary fuel injector. Fuel, gasoline; combustion-chamber-inlet static pressure, 1750 ±10 pounds per square foot absolute; combustion-chamber-inlet total temperature, 550° ±10° R.

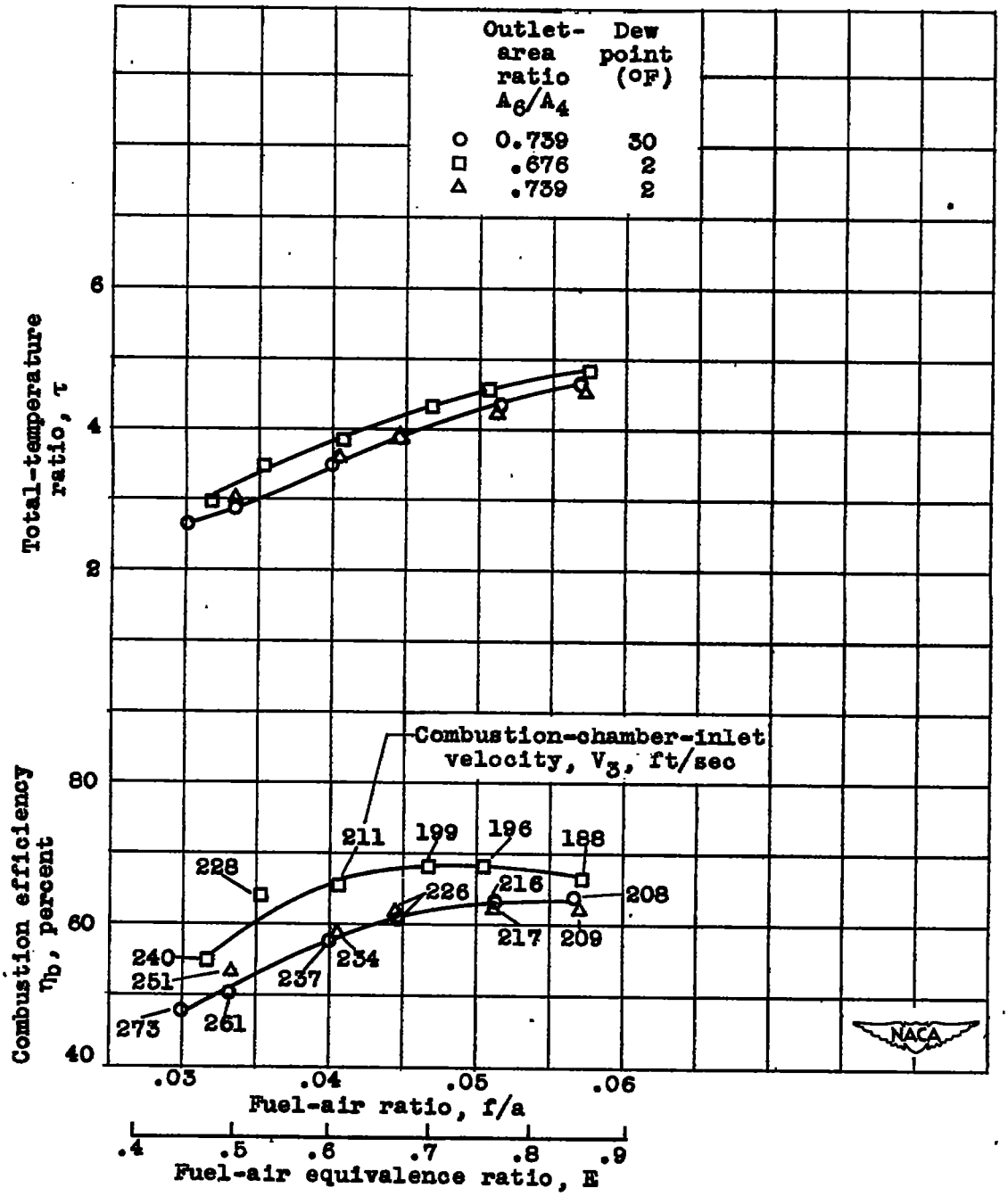

Figure 20. - Effect of fuel-air ratio on combustion efficiency and total-temperature ratio across combustion chamber with corrugated gutter burner. Fuel, gasoline; combustion-chamber-inlet static pressure, 1650 ±15 pounds per square foot absolute; combustion-chamber-inlet total temperature, 575° ±10° R.

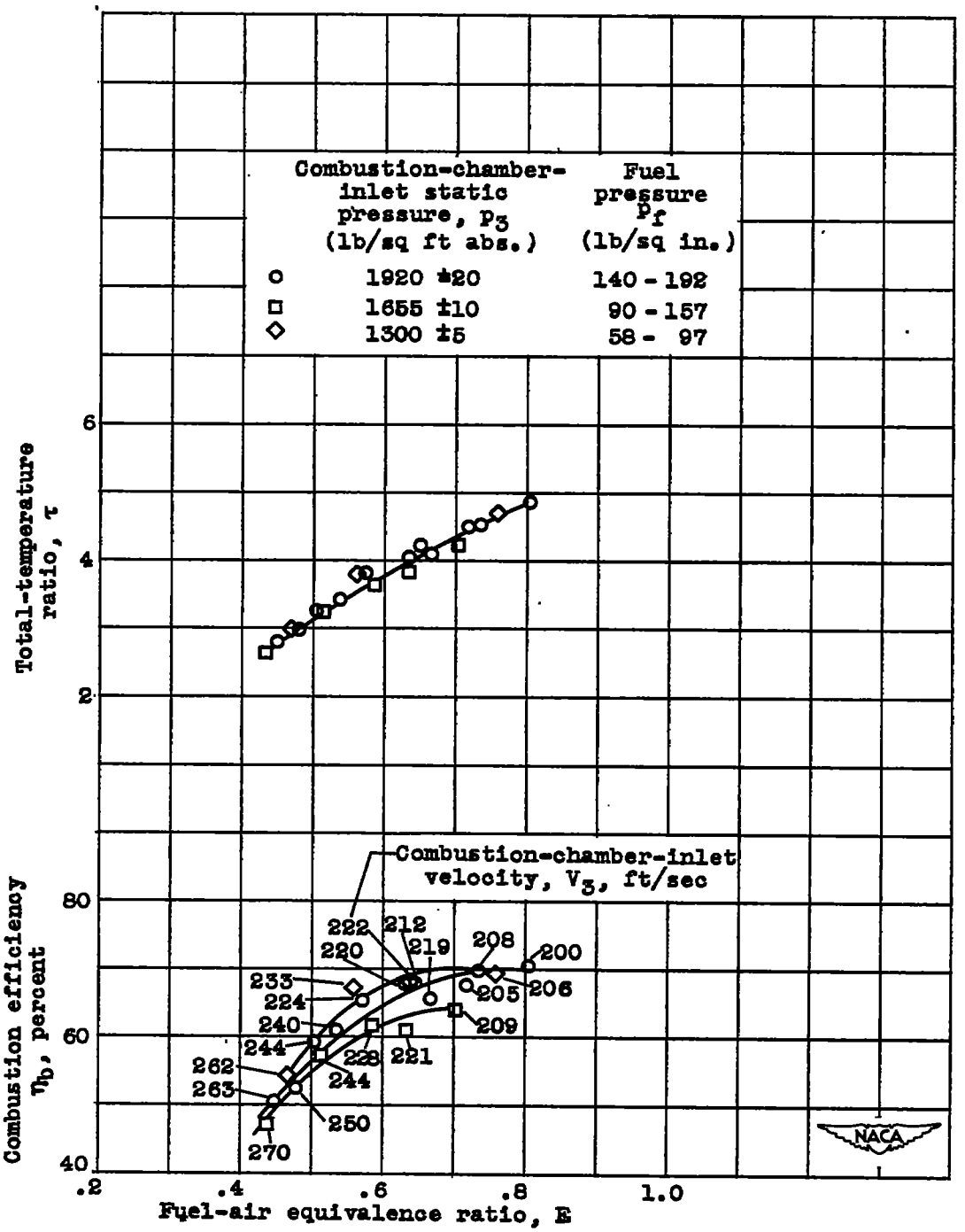

Figure 21. - Variation of combustion efficiency and total-temperature ratio across combustion chamber with fuel-air equivalence ratio for three combustion-chamber pressure levels. Corrugated gutter burner; fuel, 50-percent propylene oxide and 50-percent gasoline; combustion-chamber-inlet total temperature, 565° ±5° R; outlet-area ratio, 0.739.

[redacted]

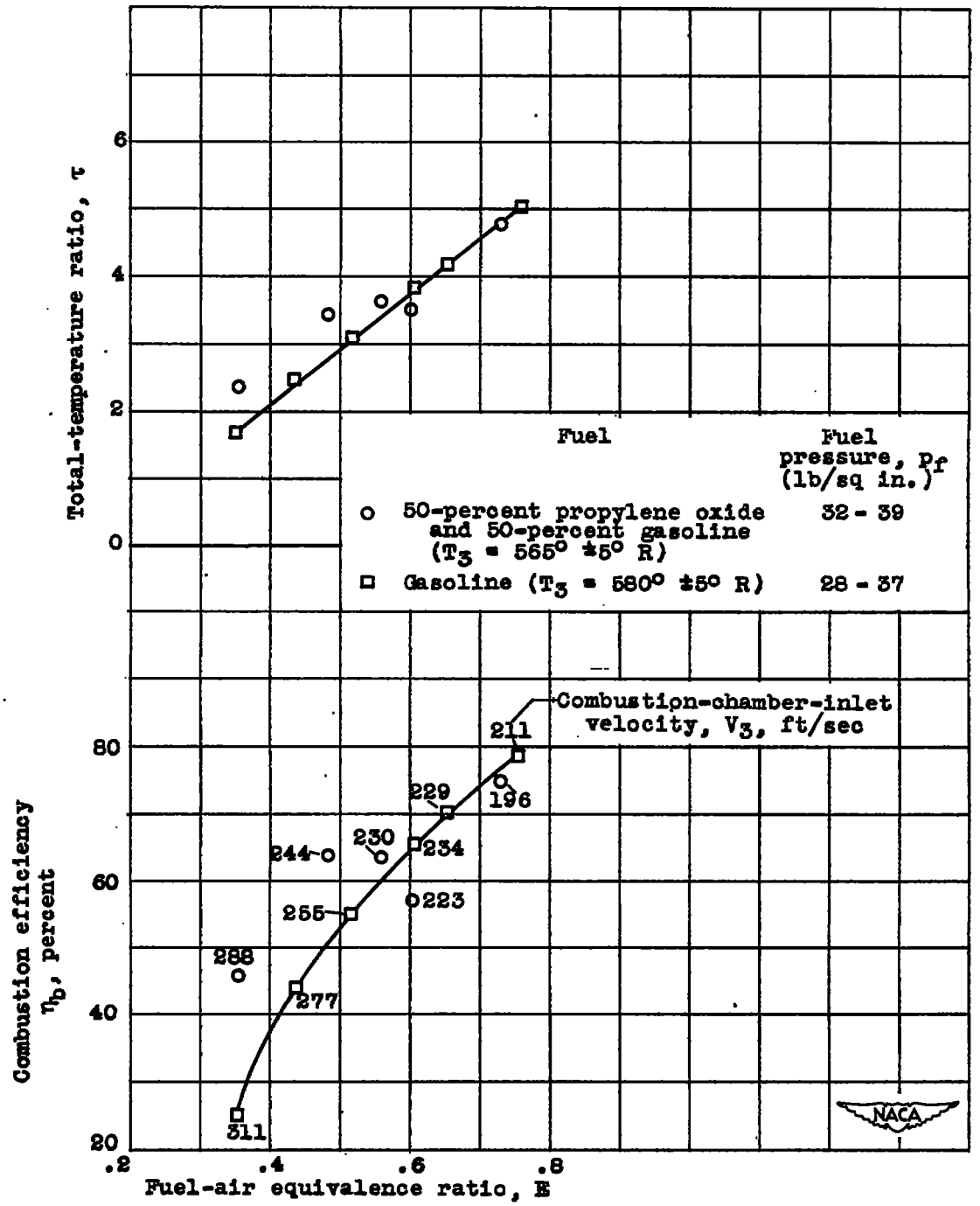

Figure 22. - Variation of combustion efficiency and total-temperature ratio across combustion chamber with fuel-air equivalence ratio for two fuels. Corrugated gutter burner; combustion-chamber-inlet static pressure, 790 ±20 pounds per square foot absolute; outlet-area ratio, 0.739; outlet not choked.

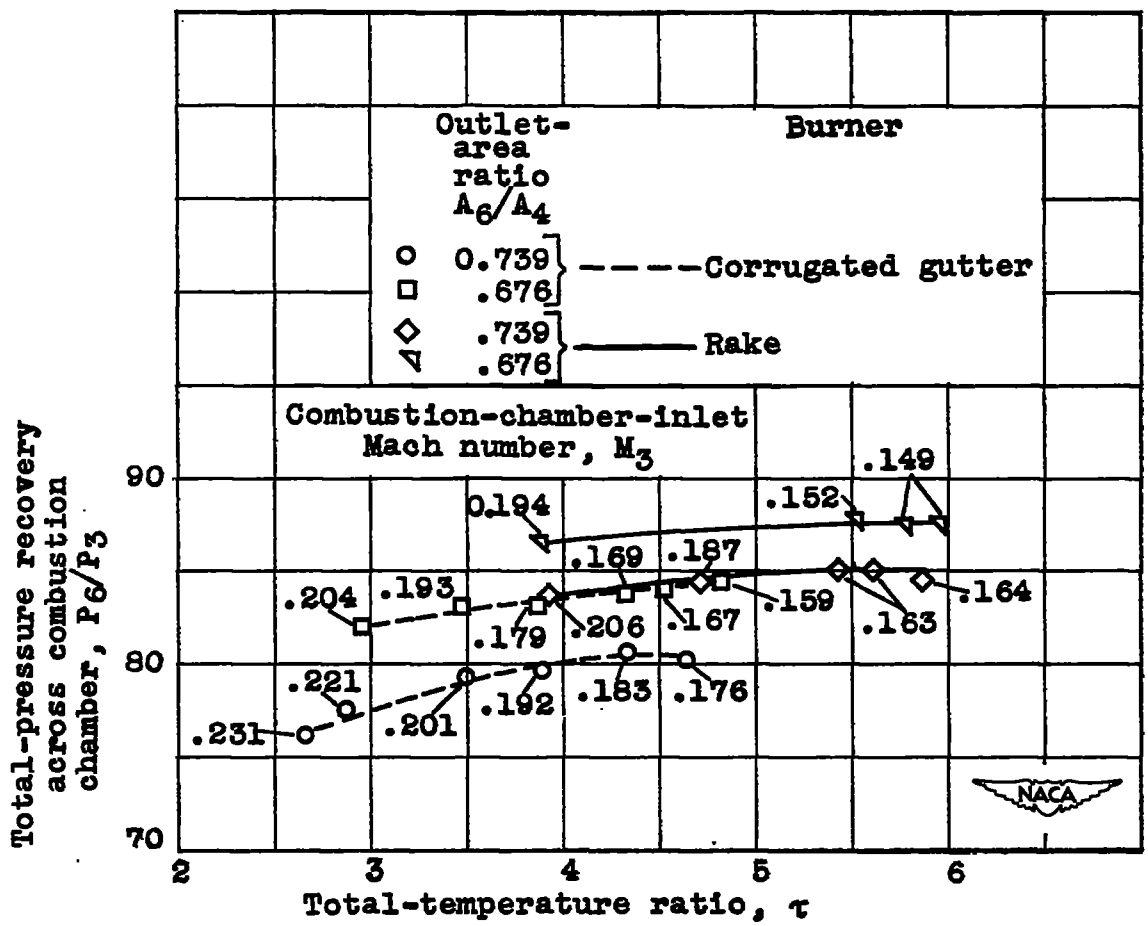

Figure 23. - Variation of pressure recovery across combustion chamber with total-temperature ratio.

NACA-Langley - 6-27-50 - 400